Supporting Information

Efficient Oxidative Coupling of Amines to Imines in Natural Sunlight using Benzothiadiazole-based Molecular Photocatalyst

Ajeet Singh[a], Bidisa Das[*b] and Saumi Ray[*a]

[a]Department of Chemistry

Birla Institute of Technology and Science (BITS), Pilani, Pilani Campus, Rajasthan 333031, India

[b]Research Institute for Sustainable Energy (RISE),

TCG-CREST, Salt Lake,700091, Kolkata, India

Email: p20200434@pilani.bits-pilani.ac.in, bidisa.das@tcgcrest.org, saumi@pilani.bits-pilani.ac.in

Corresponding Author: bidisa.das@tcgcrest.org, saumi@pilani.bits-pilani.ac.in

Table of contents

Materials

We have procured the 4,7-Dibromo-2,1,3-benzothiadiazole (98% GC), $Pd(PPh_3)_4$, 2-(aminomethyl)thiophene (98% GC), and phenylboronic acid form the TCI chemicals. CDH Fine Chemicals supplied bromobenzene (98% GC), sodium sulphate anhydrous (99%), tert-butyl alcohol, DMSO-d6, and deuterated chloroform ($CDCl_3$). We have bought benzylamine (99%), 4-fluoro benzylamine (97%), KI (99%), TEMPO, p-benzoquinone (98%), TEMP (>99%), DMPO and 2-methoxy benzylamine (98%) from Sigma-Aldrich. Merck supplied the $BaSO_4$, K_2CO_3, toluene, and acetonitrile. Hexane, methanol, and ethyl acetate were purchased from Qualigen Chemicals. Thermo-Scientific supplied 4-methyl benzylamine (98%), 2-(aminomethyl)pyridine (98%), $CuCl_2$ (99%), and 4-methoxy benzylamine (98%). All the chemicals and solvents utilized in this study were used as received without any additional purification.

Characterization

^1H & C-13 NMR spectra were recorded on the 400 MHz Brucker NMR instrument in $CDCl_3$ solvent, and data are reported in the ppm unit. HRMS study were recorded on the Agilent 6545 Q-TOF LC−MS spectrometer by using the electrospray ionization method in the positive mode in acetonitrile solvent. Perkin Elmer LAMBDA 1050+ UV/Vis/NIR spectrophotometer was used to record the solution state absorption spectra in 2nm data interval mode. Photoluminescence spectra were recorded on the Fluorolog-3 instrument. Photoluminescence lifetime studies were recorded at room temperature using the Horiba Delta Flex 01 instrument. Gas-chromatography study for the catalysis was done using the Shimadzu GC-2014 with an FID detector and column RTX-5 in an autosampler mode using 0.5µl injection volume and bromobenzene as an internal standard. EPR/ESR measurements were recorded using the Bruker A300-9.5/12/S/W at room temperature using the UV-visible 100W Hg lamp as a light irradiation source. CH instrument (CHI601E) was used to record the cyclic voltammetry studies using the NBu_4PF_6 as an electrolyte in acetonitrile, and the Ag/AgCl as a reference electrode, platinum wire as a counter electrode, glassy carbon electrode was used as a working electrode. Intensity of the sunlight was measured using the Newport power meter 843-R at 500nm wavelength.

Computational Methodology

All studies for the photocatalyst and related complexes were performed using density functional theory (DFT) as implemented in the GAUSSIAN 16, suite of *ab initio* quantum chemistry program.[1] Geometry optimizations and vibrational frequency calculations were done using hybrid B3LYP[2-4] functional with the double-zeta quality 6-311+G** basis set for all atoms. The default SCF and geometry convergence criteria were used, and no symmetry constraints were imposed for the structural optimizations. Harmonic frequency analysis was employed to characterize the stationary points as stable structures. The frontier molecular orbitals and the energy gap between the highest occupied molecular orbital (HOMO) and lowest unoccupied molecular orbital (LUMO) and molecular electrostatic potential are calculated using B3LYP functional. Calculation of atomic charges were done using the Merz-Singh-Kollman approach[5, 6] which gives more accurate results compared to conventional Mulliken scheme.

For any chemical reaction, Reactants → Products, the Gibb's free energy of reaction is calculated as $\Delta G_{reaction} = \Sigma_{products} G - \Sigma_{reactants} G$, where ΔG represents the sum of electronic and thermal free energies of the corresponding species. To model the solution phase of the photocatalyst and photocatalyst complexes, we have conducted full optimization followed by vibrational frequency calculation in solvent using the self-consistent reaction field (SCRF) method and density-based model (SMD)[7, 8] employing implicit solvation with ACN as a solvent. The binding energy (E_{bind}) of the adsorbates to Ph-BT-Ph molecule is calculated using the equation below:

$$E_{bind} = E_{[Ph\text{-}BT\text{-}Ph]\text{-}adsorbate} - (E_{Ph\text{-}BT\text{-}Ph} + E_{adsorbate})$$

Here $E_{[Ph\text{-}BT\text{-}Ph]\text{-}adsorbate}$ represents the energy of the Ph-BT-Ph bound to the respective adsorbate molecule, BNA or Oxygen, the energy of the pristine Ph-BT-Ph is $E_{Ph\text{-}BT\text{-}Ph}$ and $E_{adsorbate}$ gives the energy of the free BNA or O_2 as applicable respectively. The calculations of excited states on the stable ground–state geometry was carried out by using time–dependent (TD) formalism in DFT (TD–DFT) and the TD-DFT spectrum has been plotted. We also performed structural optimizations on few excited states explored from TD-DFT and investigated their interactions with the reactants.

^{1}H NMR (400 MHz, $CDCl_3$)

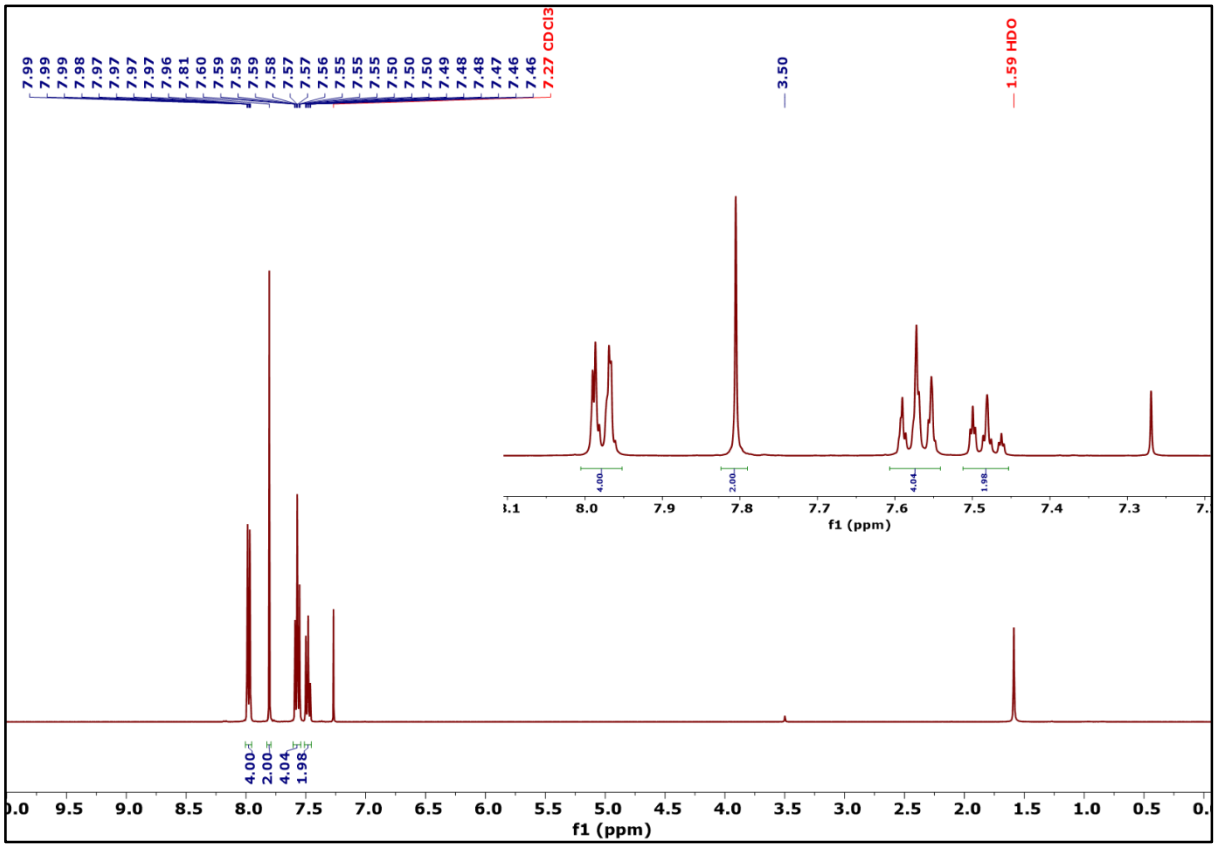

Figure S1 ^{1}H NMR of Ph-BT-Ph

^{13}C NMR (101 MHz, $CDCl_3$)

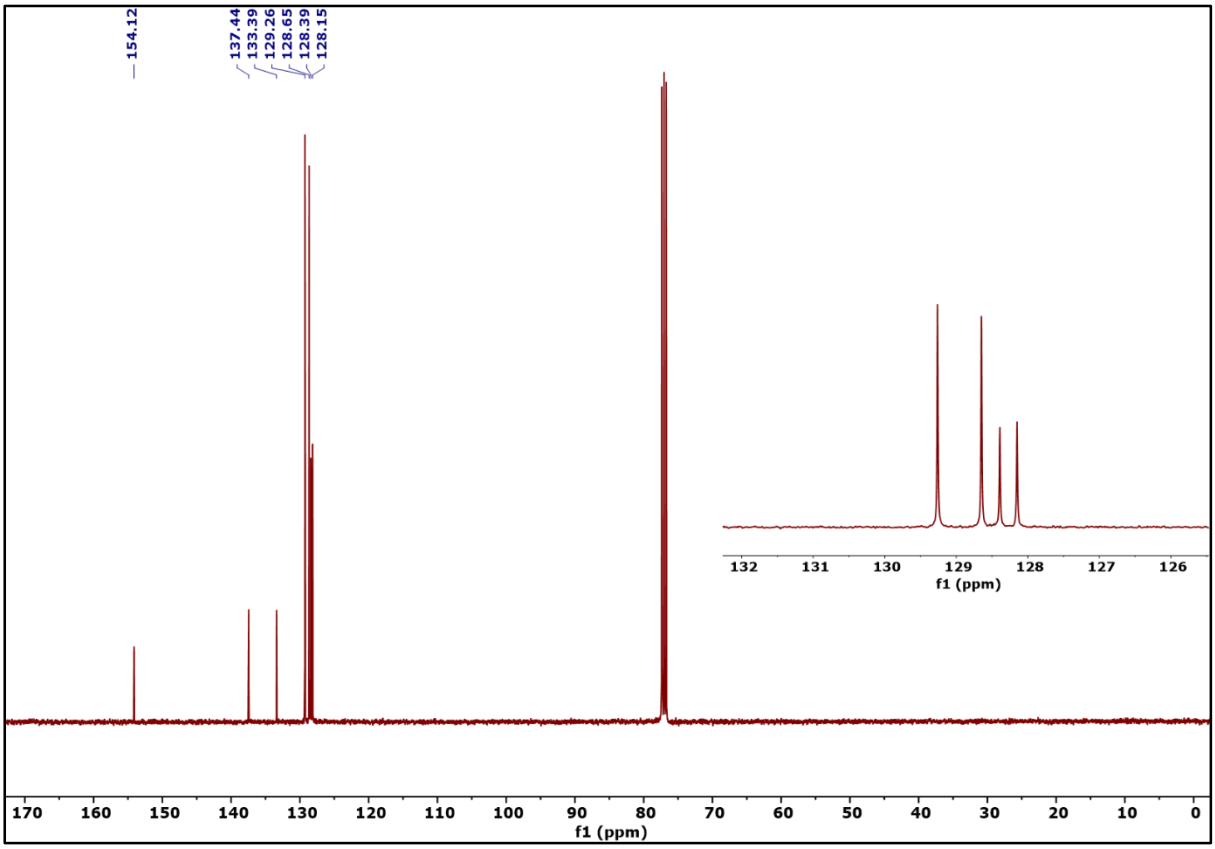

Figure S2 ^{13}C NMR of Ph-BT-Ph

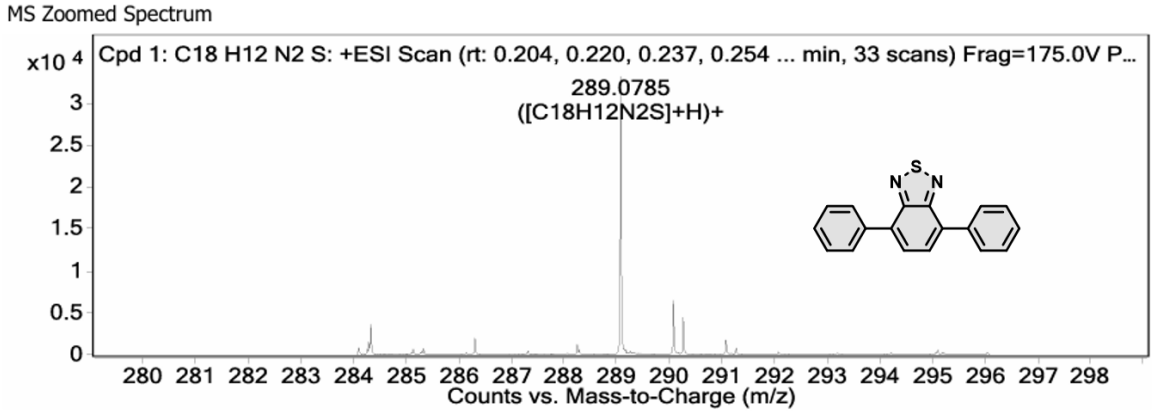

MS Spectrum Peak List

m/z	*Calc m/z*	Diff(ppm)	z	Abund	Formula	Ion
289.0785	289.0794	3.04	1	33298.6	C18H12N2S	(M+H)+
290.0815	290.0824	3.26	1	6744.17	C18H12N2S	(M+H)+
291.0774	291.0785	3.62	1	1798.1	C18H12N2S	(M+H)+

Figure S3 HRMS spectra of Ph-BT-Ph

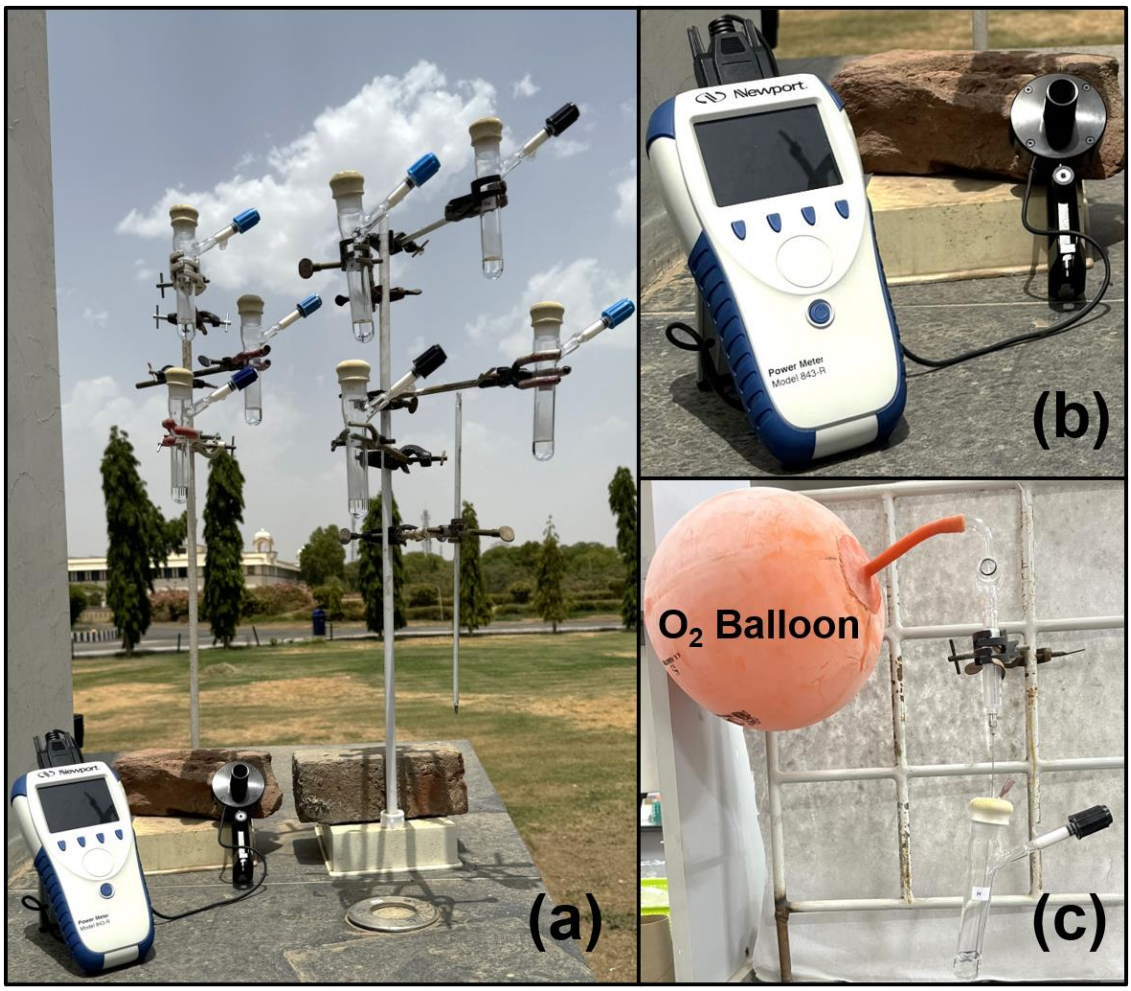

Figure S4 (a) Digital photograph of the reaction setup in natural sunlight **(b)** Newport power meter for intensity measurement **(c)** O_2 purging setup.

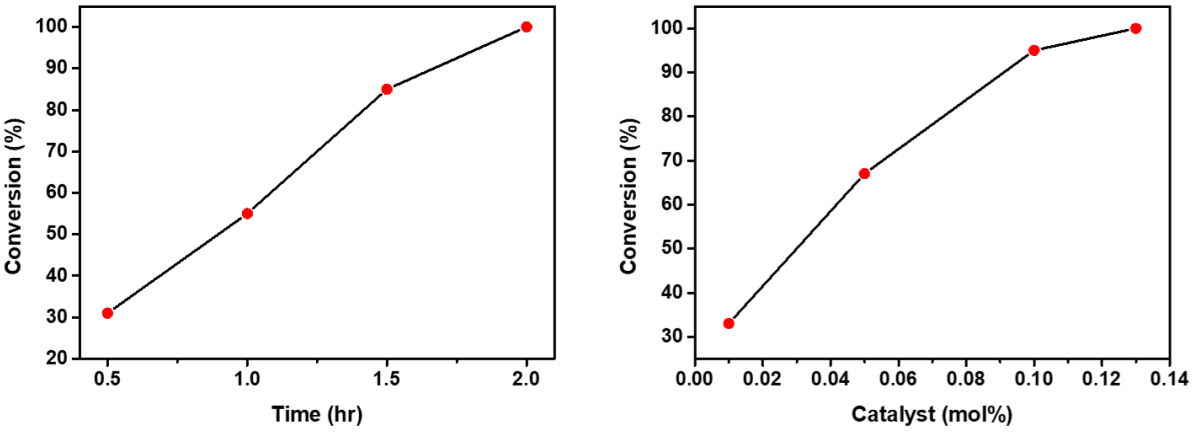

Figure S5 Optimization of reaction time and amount of catalyst result for oxidative coupling of amine to imine.

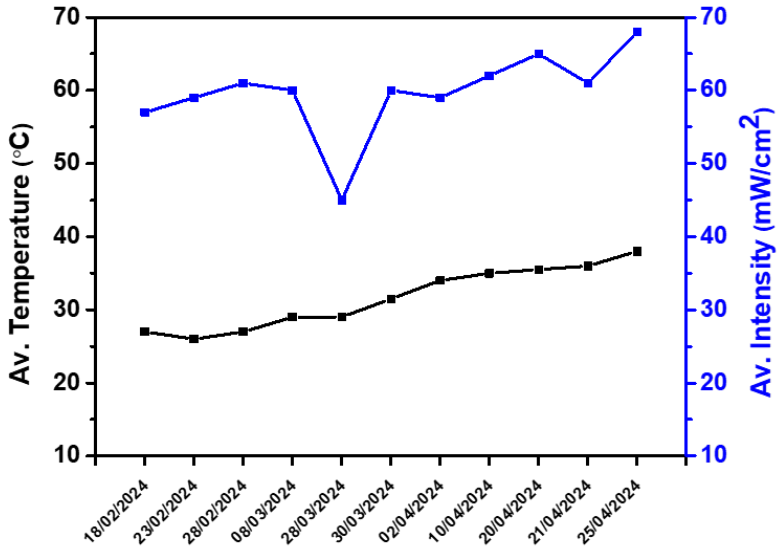

Figure S6 Average intensity and temperature of sunlight during the reaction time on that day.

Table S1 GC retention time of reactant and product.

Reactant	Retention time of reactant (min)	Retention time of product (min)
1a	5.813	15.371
1b	7.989	16.830
1c	6.159	15.273
1d	10.544	20.062
1e	10.150	18.716
1f	5.925	15.669
1g	6.715	15.754

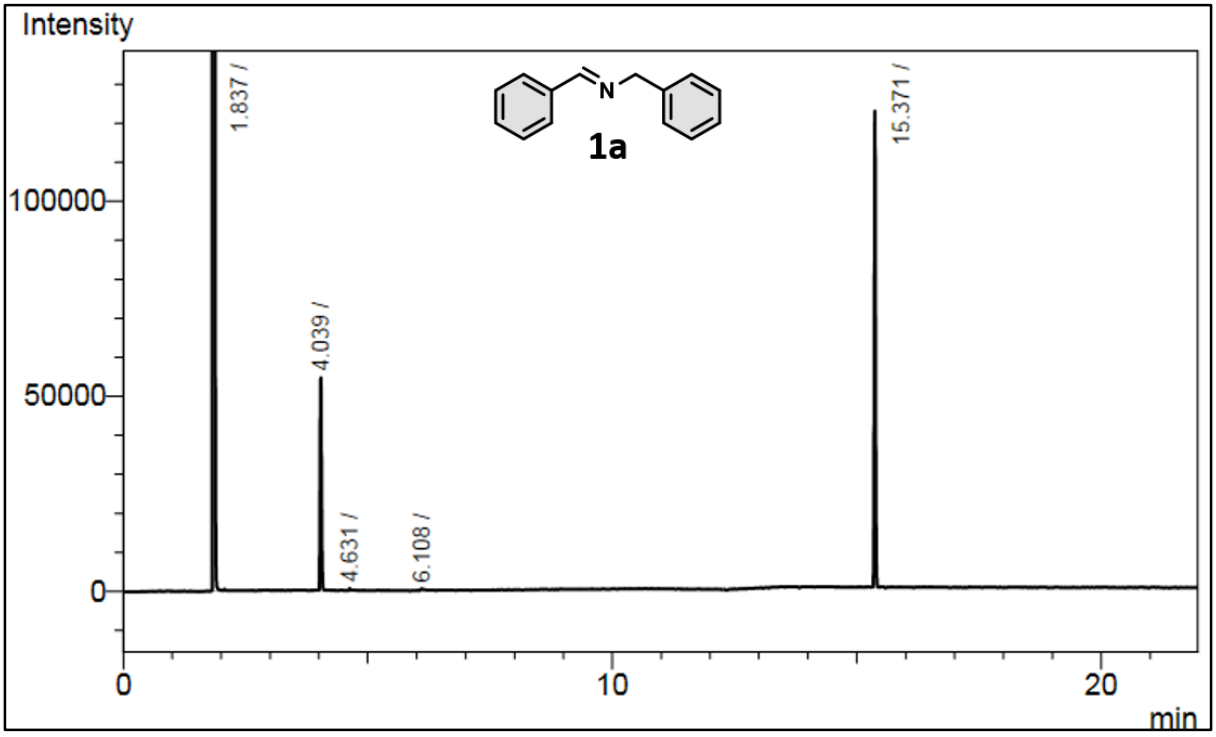

Figure S7 GC chromatogram of 1a reaction mixture. (Rt. of ACN is 1.837 min & bromobenzene is 4.039 min)

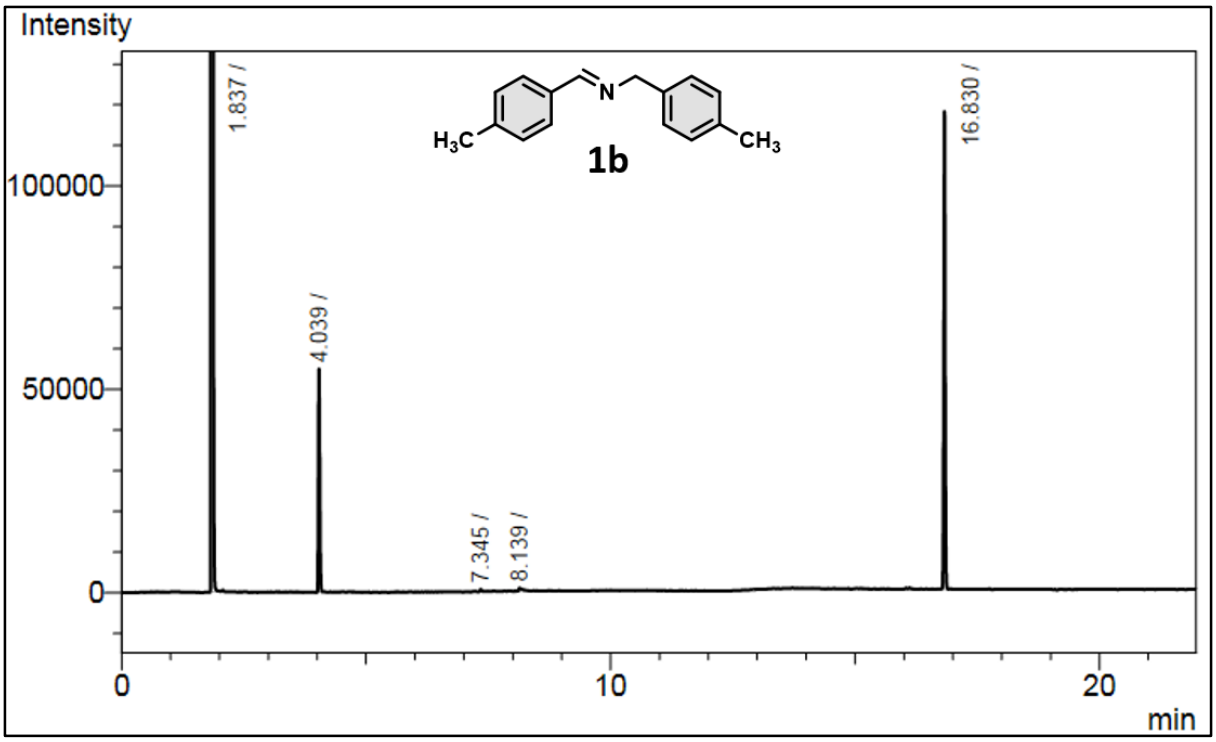

Figure S8 GC chromatogram of 1b reaction mixture. (Rt. of ACN is 1.837 min & bromobenzene is 4.039 min)

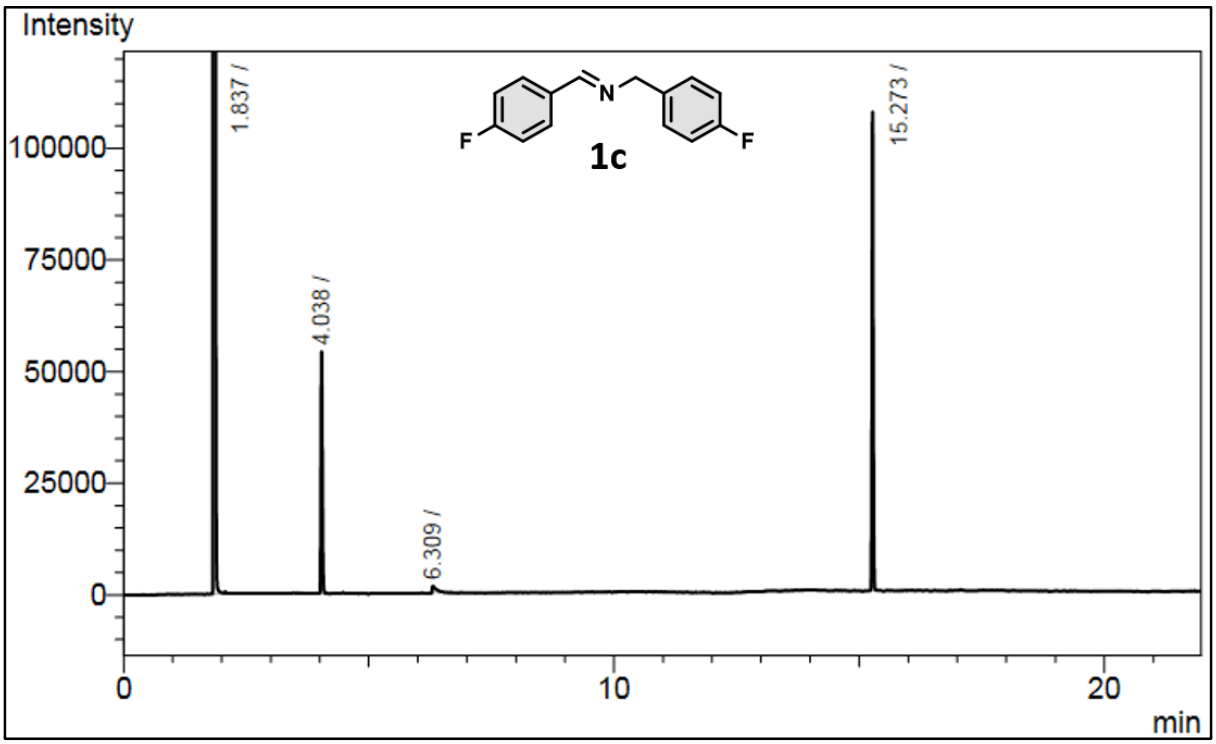

Figure S9 GC chromatogram of 1c reaction mixture. (Rt. of ACN is 1.837 min & bromobenzene is 4.038 min)

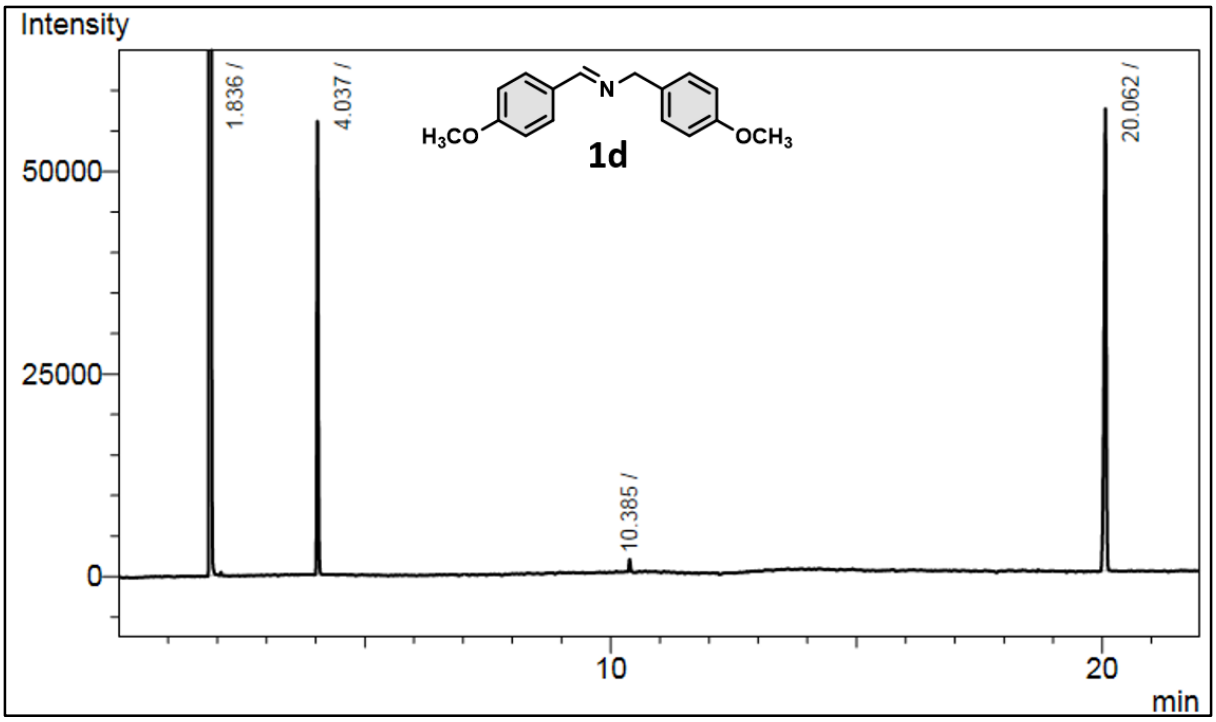

Figure S10 GC chromatogram of 1d reaction mixture. (Rt. of ACN is 1.836 min & bromobenzene is 4.037 min)

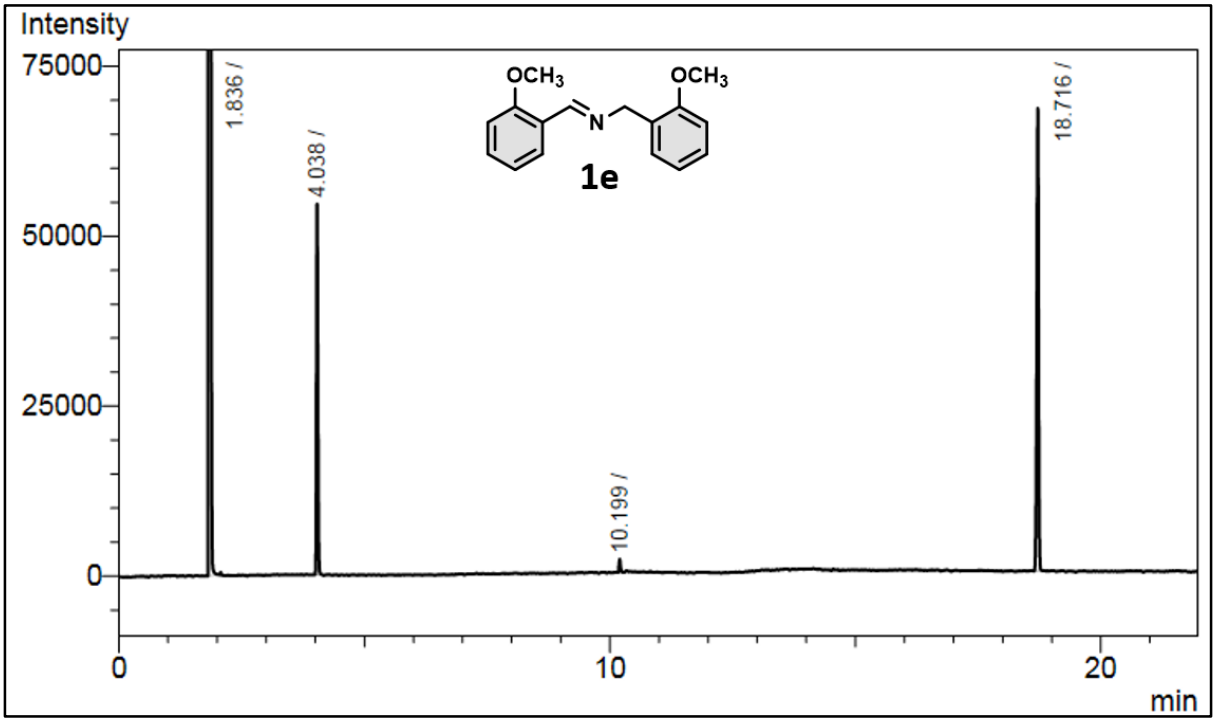

Figure S11 GC chromatogram of 1e reaction mixture. (Rt. of ACN is 1.836 min & bromobenzene is 4.038 min)

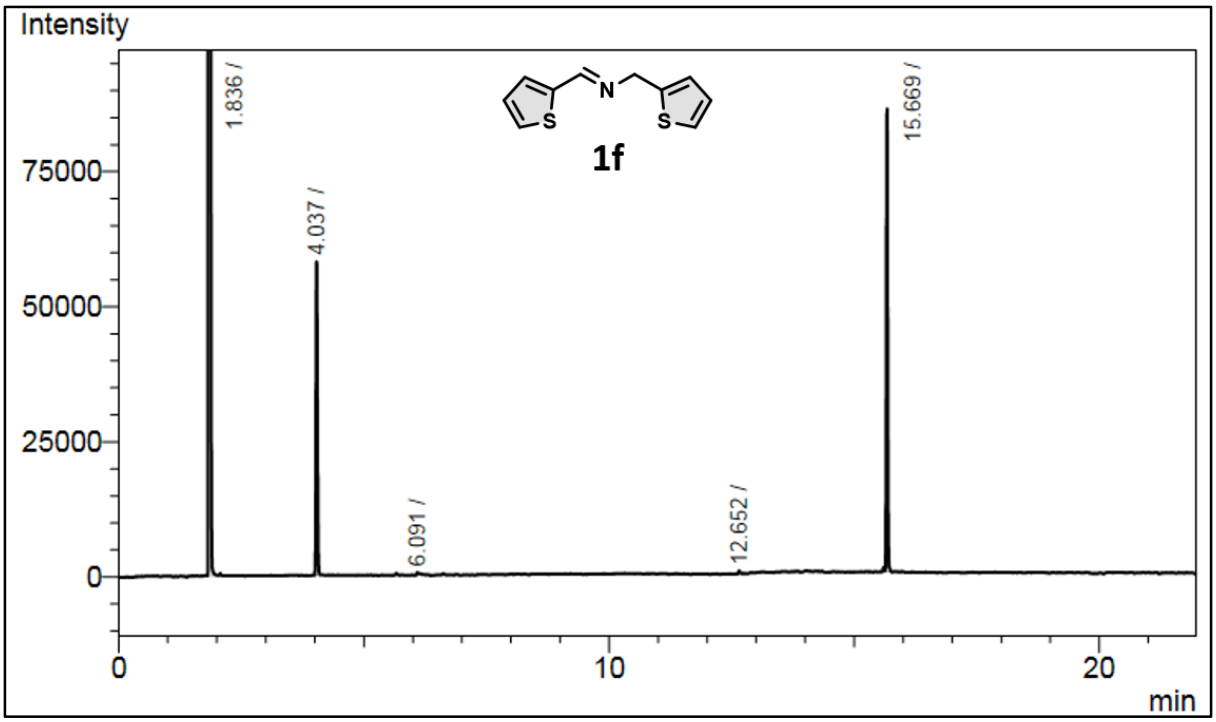

Figure S12 GC chromatogram of 1f reaction mixture. (Rt. of ACN is 1.836 min & bromobenzene is 4.037 min)

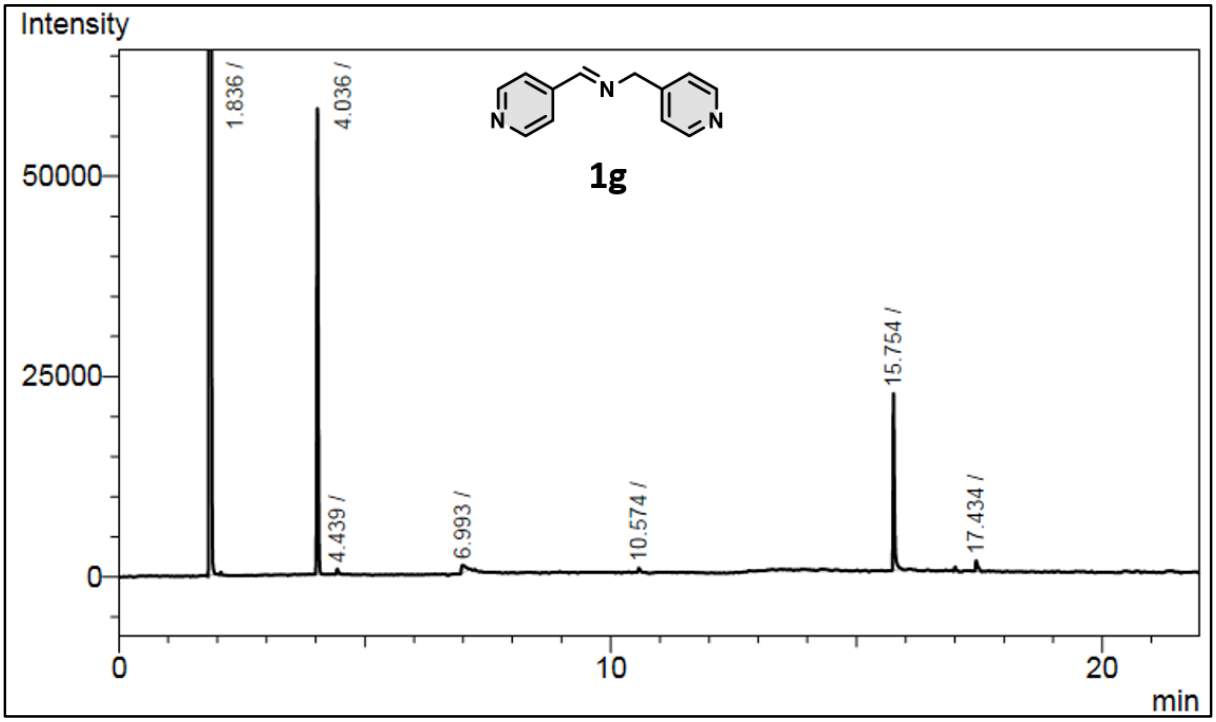

Figure S13 GC chromatogram of 1g reaction mixture. (Rt. of ACN is 1.836 min & bromobenzene is 4.036 min)

^{1}H NMR (400 MHz, $CDCl_3$)

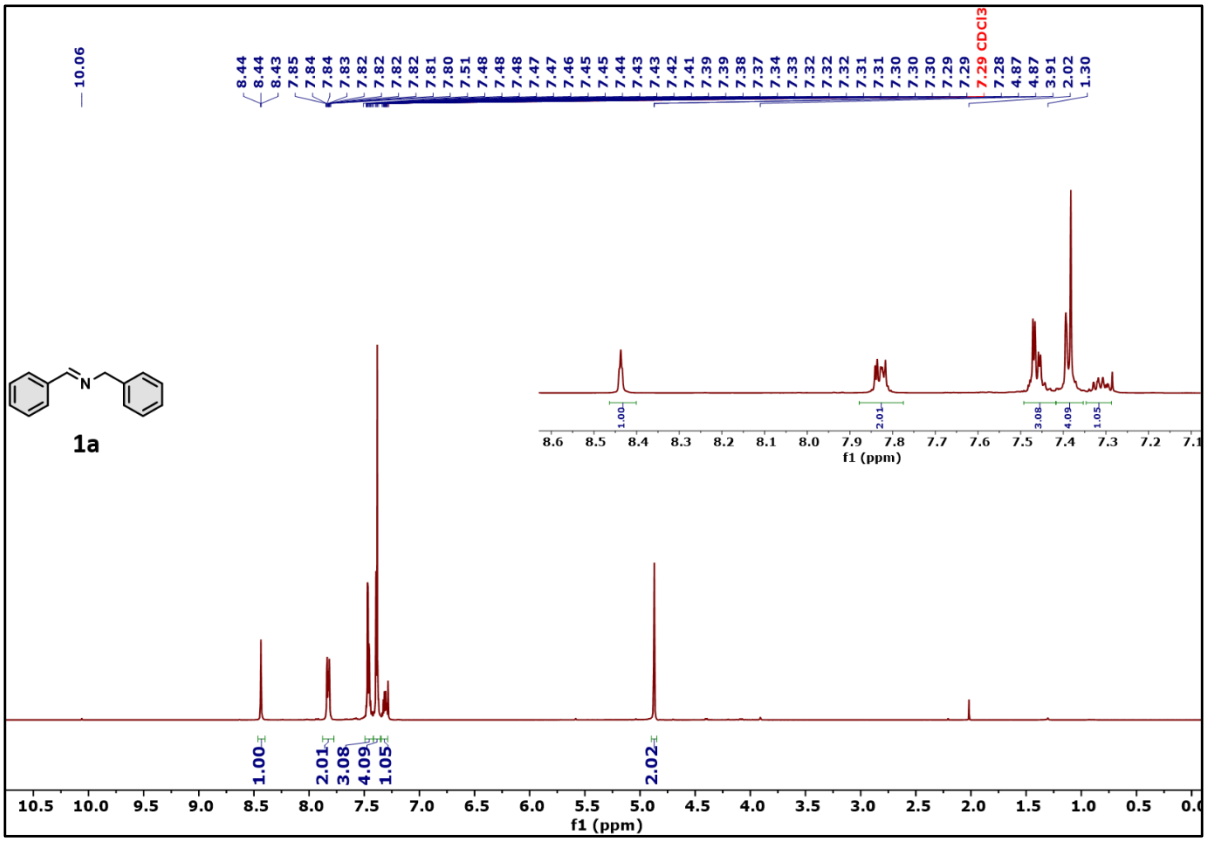

Figure S14 ^{1}H NMR spectra of 1a reaction mixture.

^{13}C NMR (101 MHz, $CDCl_3$)

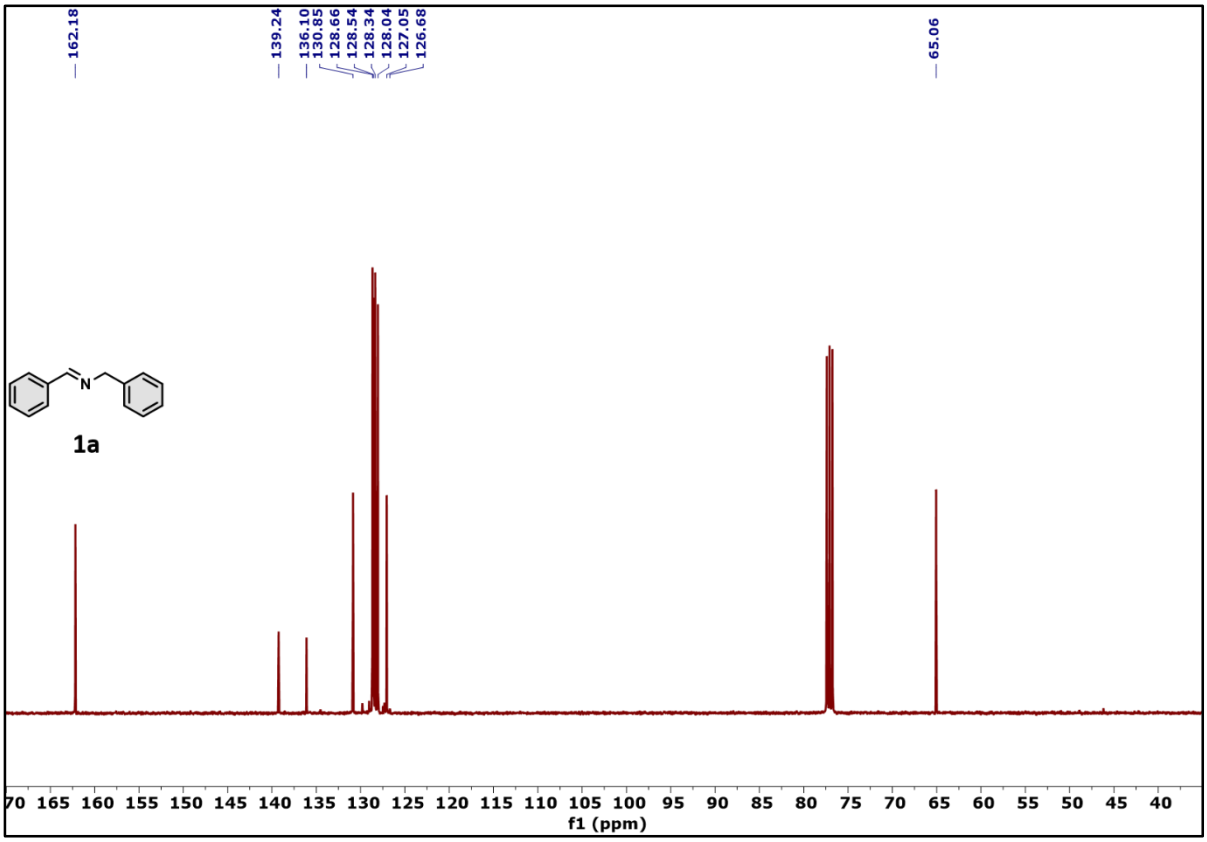

Figure S15 ^{13}C NMR spectra of 1a reaction mixture.

^{1}H NMR (400 MHz, $CDCl_3$)

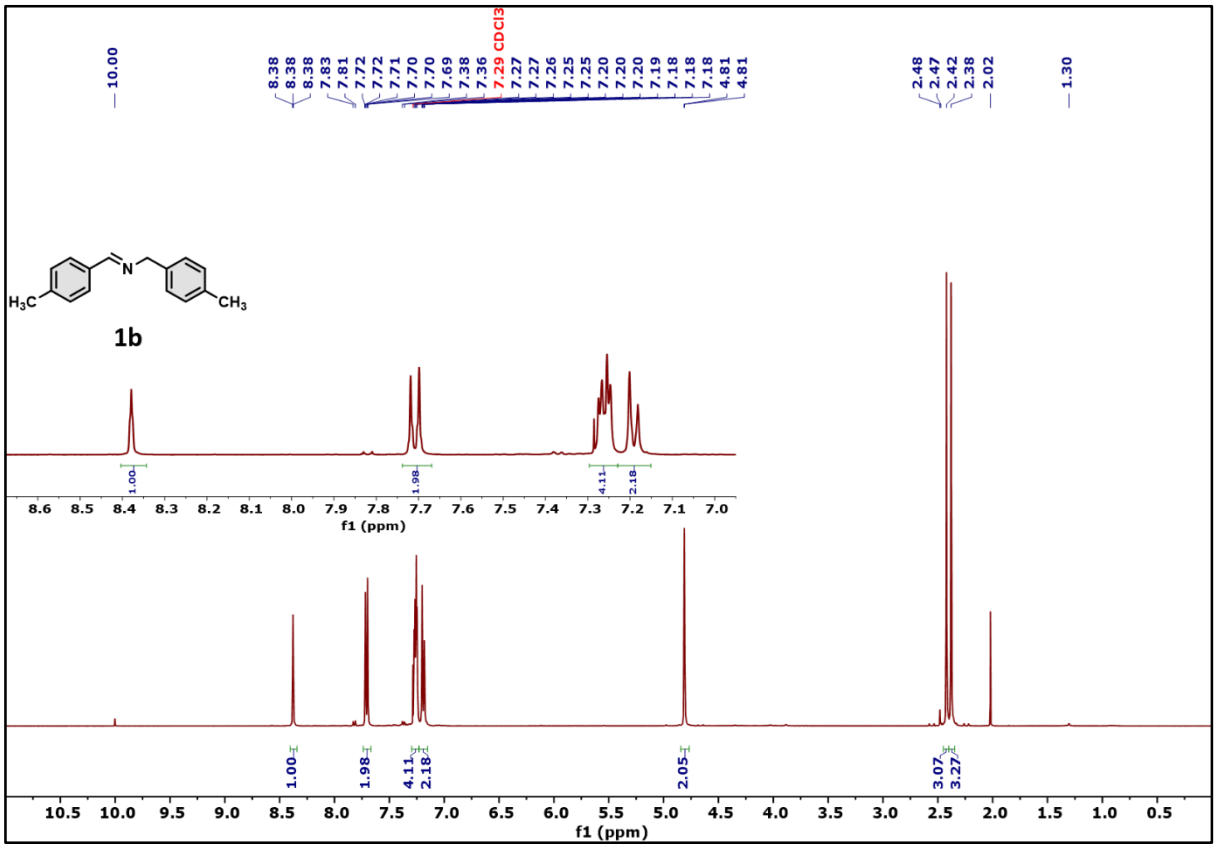

Figure S16 ^{1}H NMR spectra of 1b reaction mixture.

^{13}C NMR (101 MHz, $CDCl_3$)

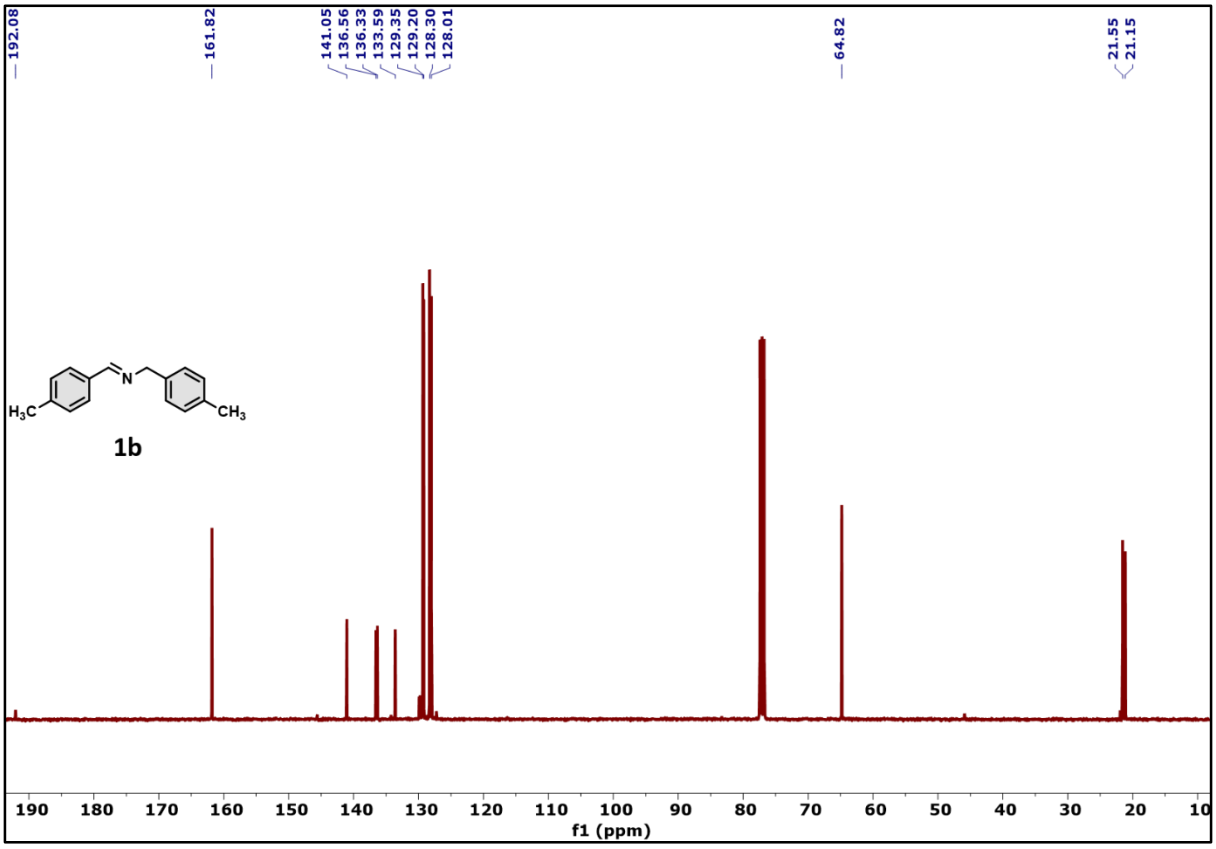

Figure S17 ^{13}C NMR spectra of 1b reaction mixture.

^{1}H NMR (400 MHz, $CDCl_3$)

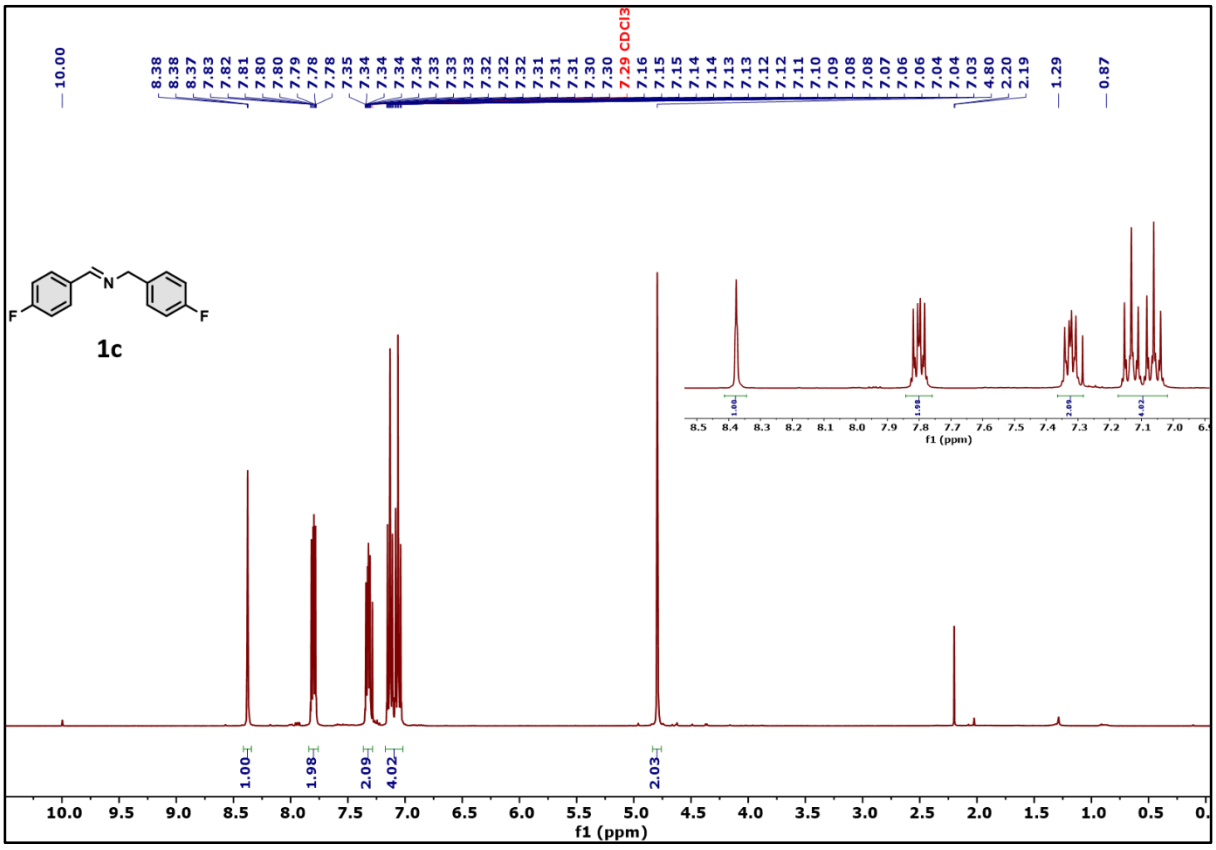

Figure S18 ^{1}H NMR spectra of 1c reaction mixture.

^{13}C NMR (101 MHz, $CDCl_3$)

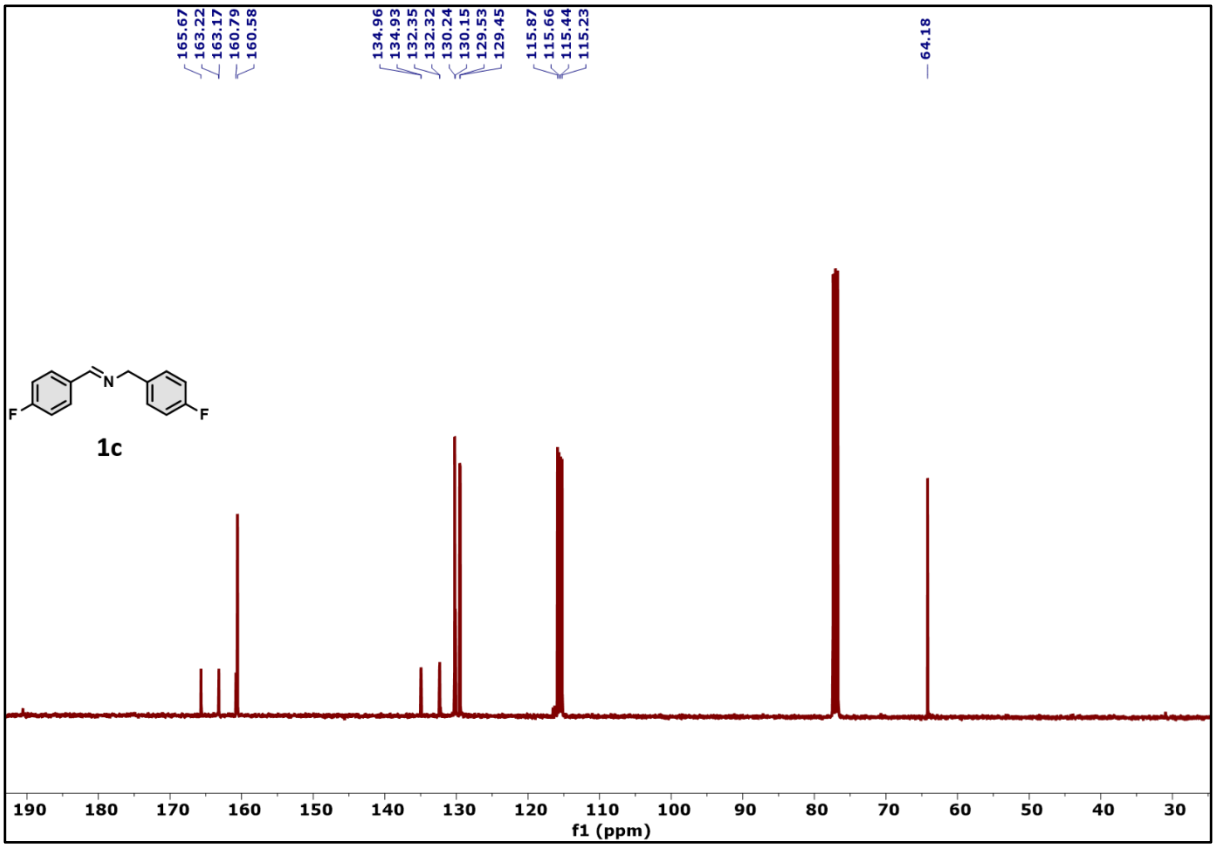

Figure S19 ^{13}C NMR spectra of 1c reaction mixture.

^{1}H NMR (400 MHz, $CDCl_3$)

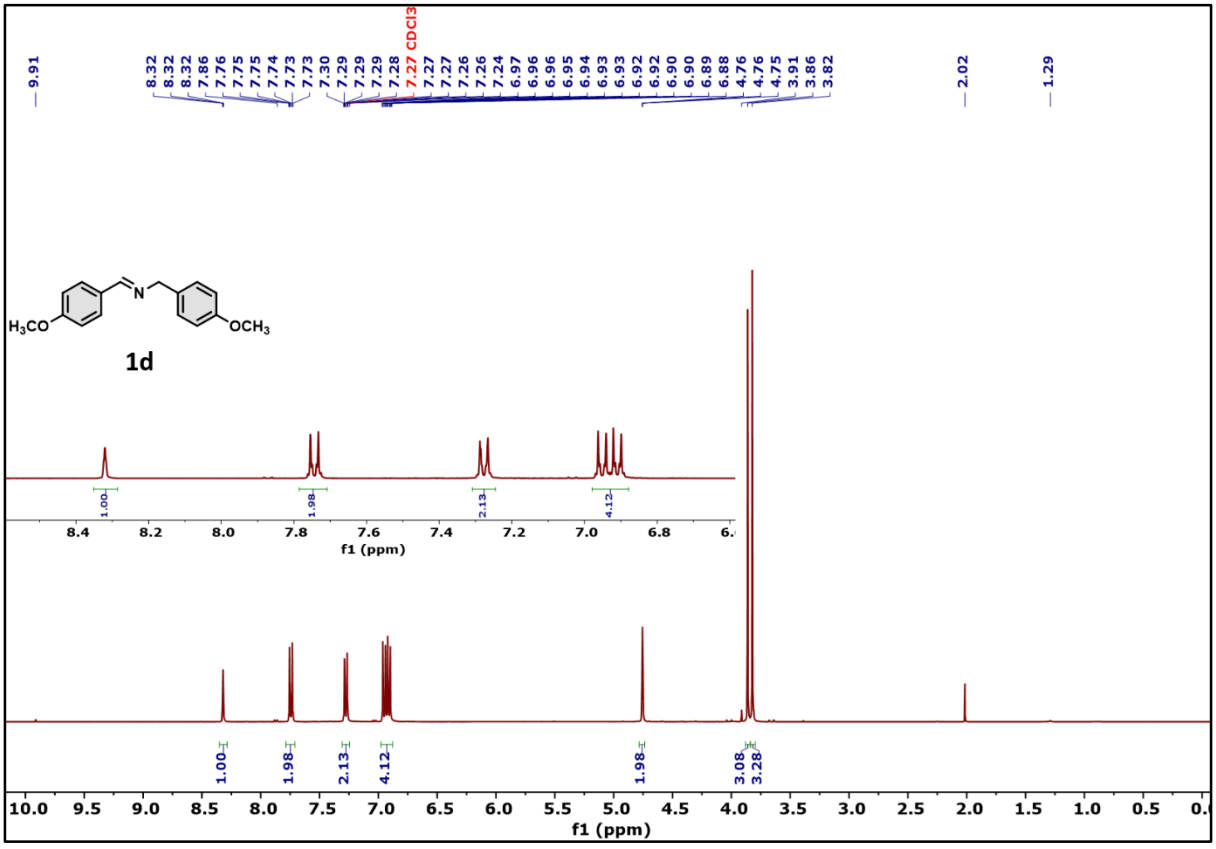

Figure S20 ^{1}H NMR spectra of 1d reaction mixture.

^{13}C NMR (101 MHz, $CDCl_3$)

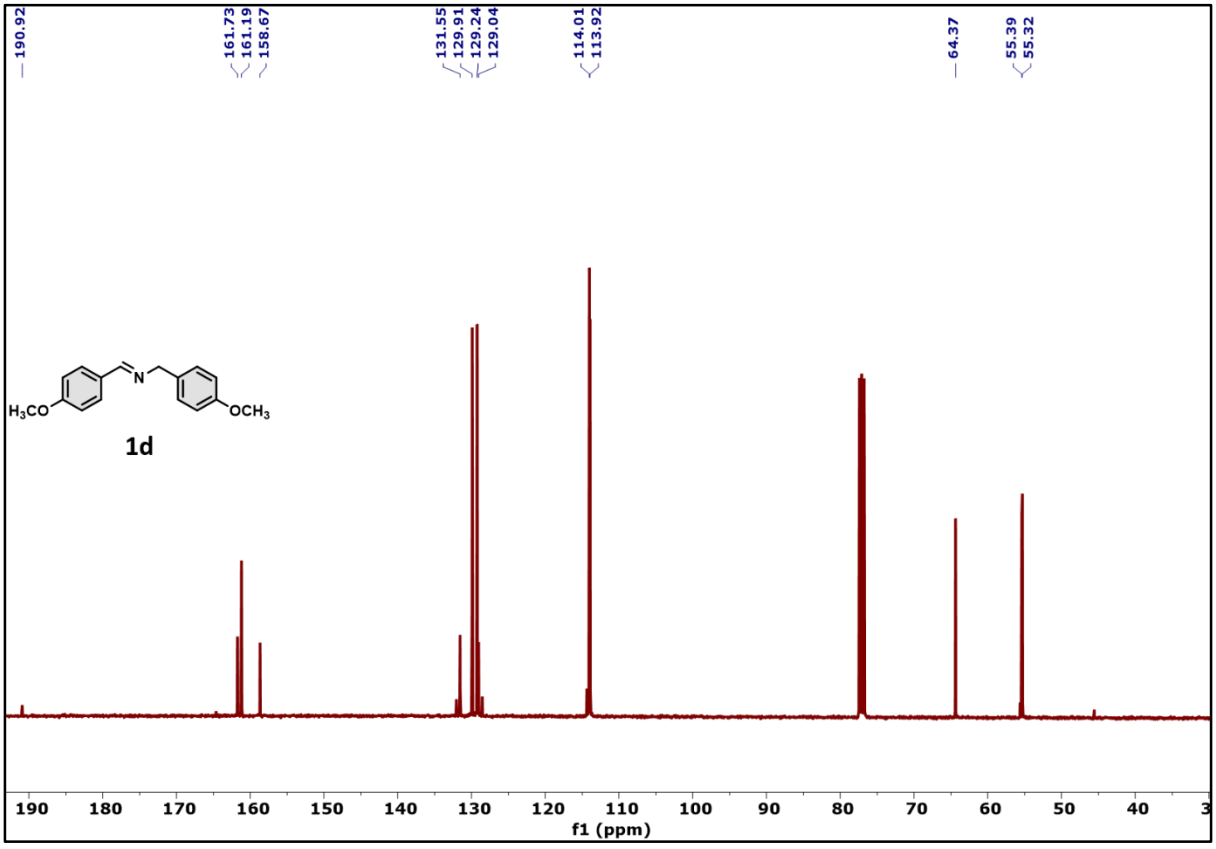

Figure S21 ^{13}C NMR spectra of 1d reaction mixture.

^{1}H NMR (400 MHz, $CDCl_3$)

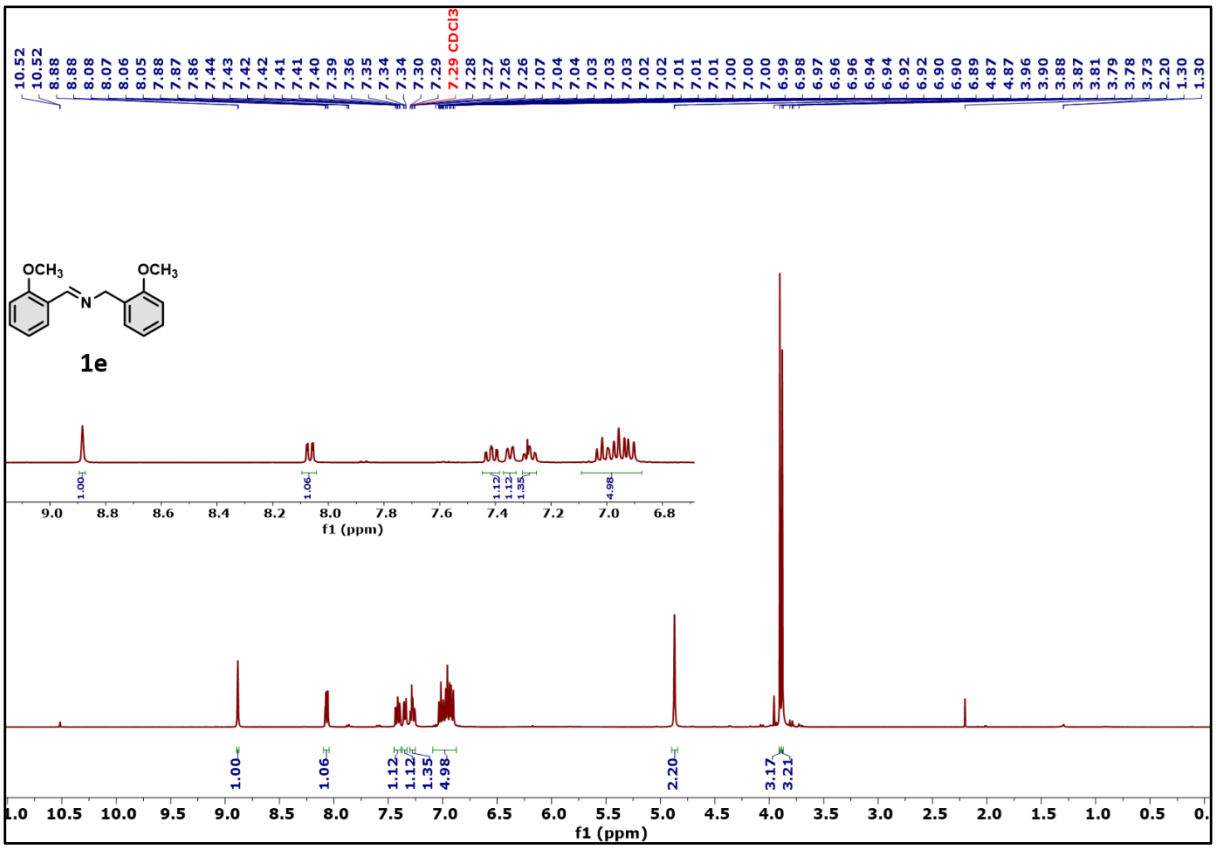

Figure S22 ^{1}H NMR spectra of 1e reaction mixture.

^{13}C NMR (101 MHz, $CDCl_3$)

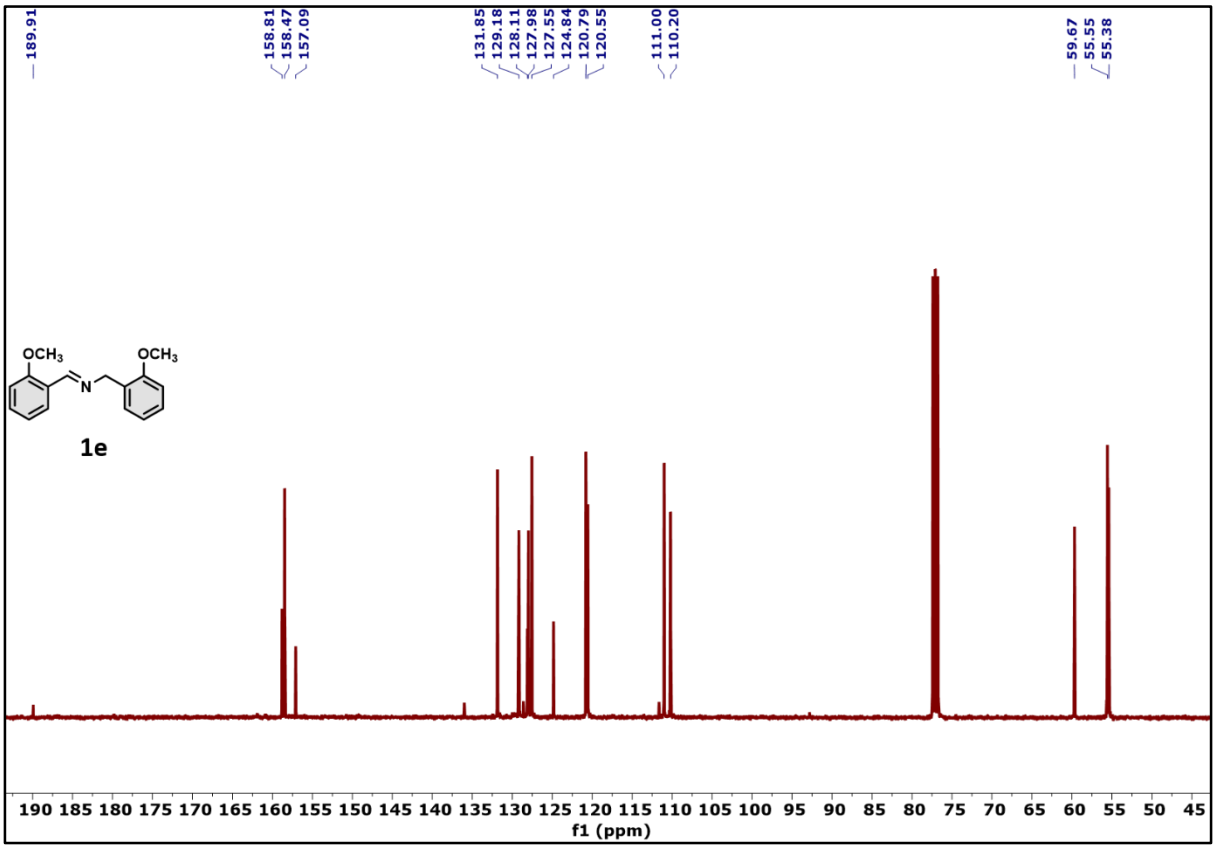

Figure S23 ^{13}C NMR spectra of 1e reaction mixture.

^{1}H NMR (400 MHz, DMSO-d6)

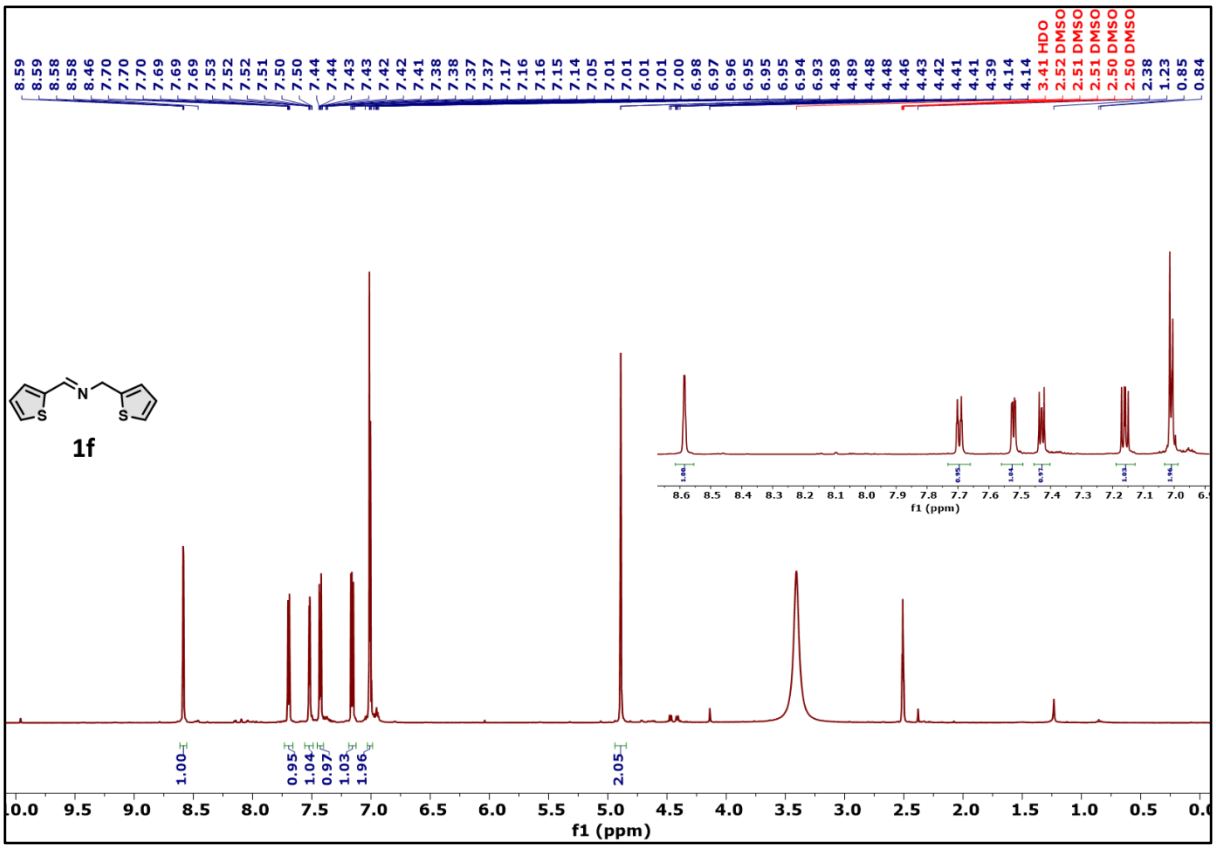

Figure S24 ^{1}H NMR spectra of 1f reaction mixture.

^{13}C NMR (101 MHz, DMSO-d6)

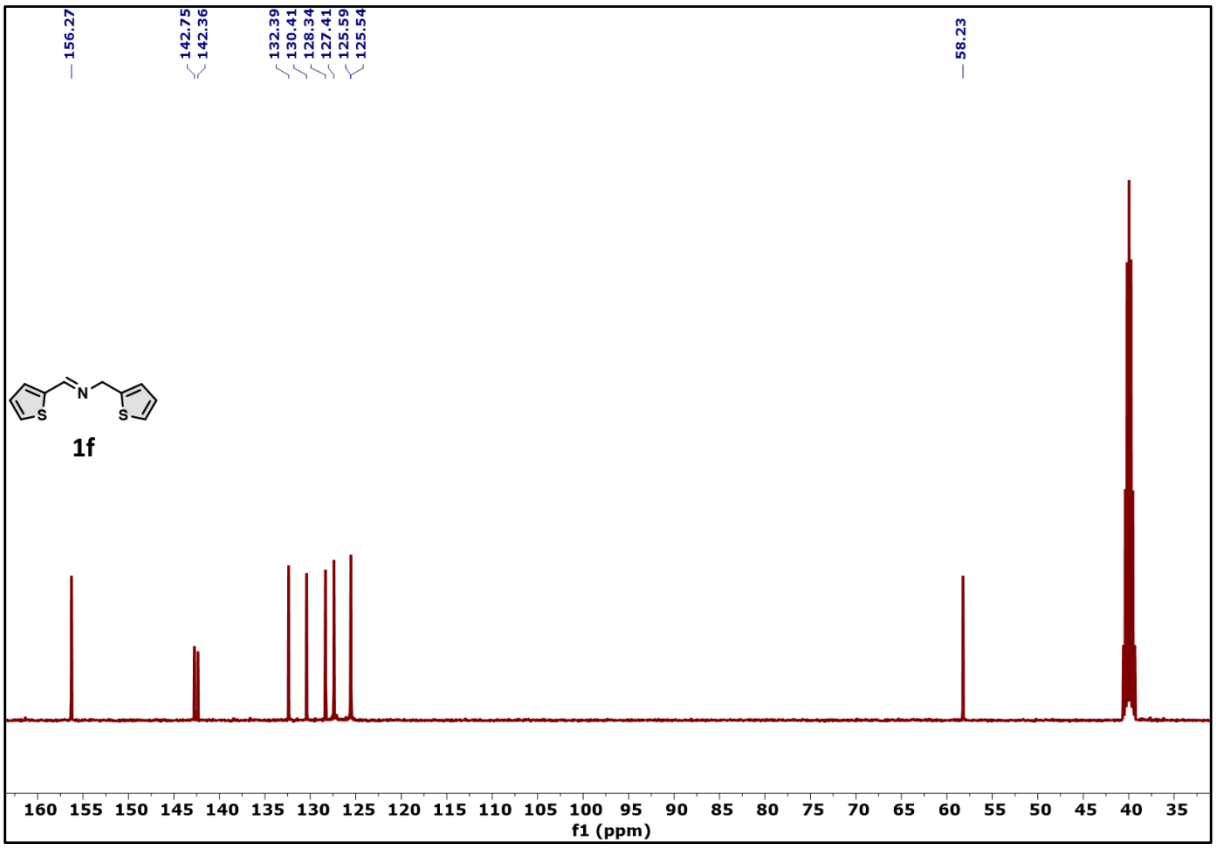

Figure S25 ^{13}C NMR spectra of 1f reaction mixture.

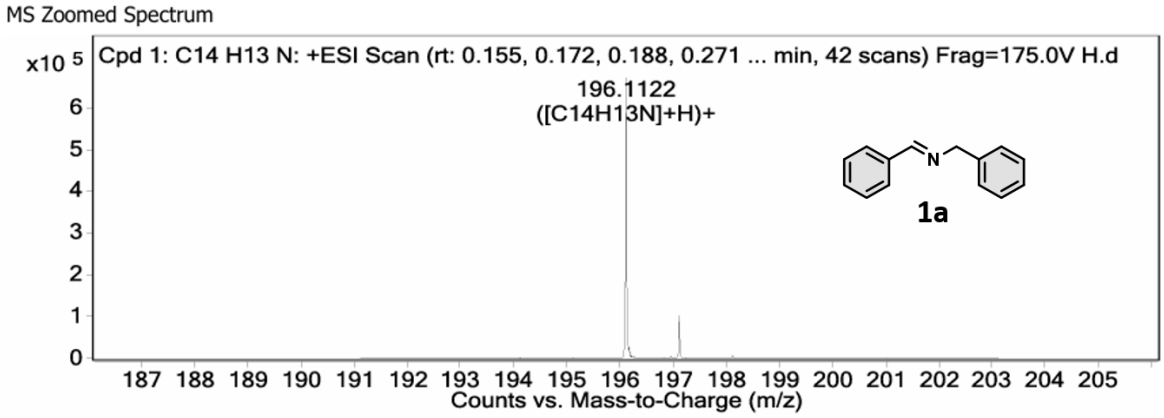

MS Spectrum Peak List

m/z	*Calc m/z*	Diff(ppm)	z	Abund	Formula	Ion
196.1122	196.1121	-0.54	1	682509.31	C14H13N	(M+H)+
197.1154	197.1153	-0.6	1	103432.64	C14H13N	(M+H)+
198.1189	198.1185	-1.65	1	8121.99	C14H13N	(M+H)+

Figure S26 HRMS data for 1a

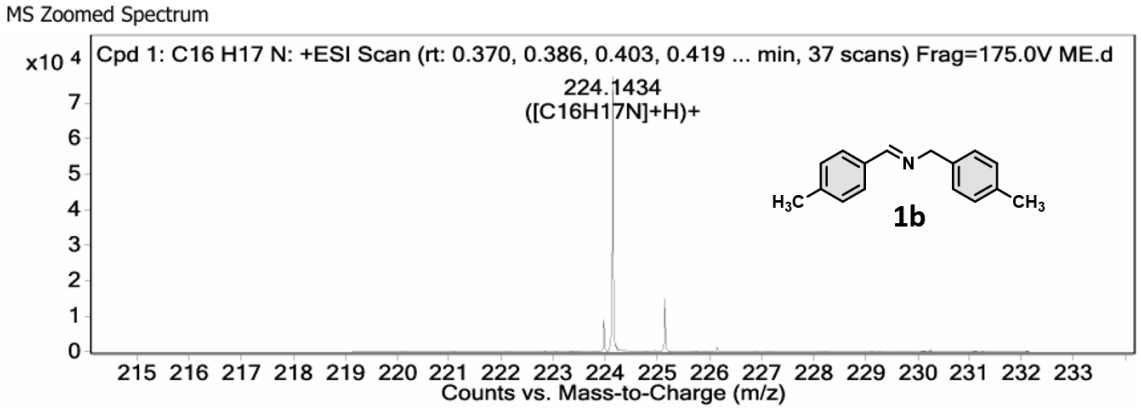

MS Spectrum Peak List

m/z	*Calc m/z*	Diff(ppm)	z	Abund	Formula	Ion
224.1434	224.1434	0.06	1	81855.77	C16H17N	(M+H)+
225.1466	225.1466	0.25	1	15177.65	C16H17N	(M+H)+
226.1498	226.1499	0.53	1	1330.11	C16H17N	(M+H)+
227.1467	227.1531	28.44	1	74.71	C16H17N	(M+H)+

Figure S27 HRMS data for 1b

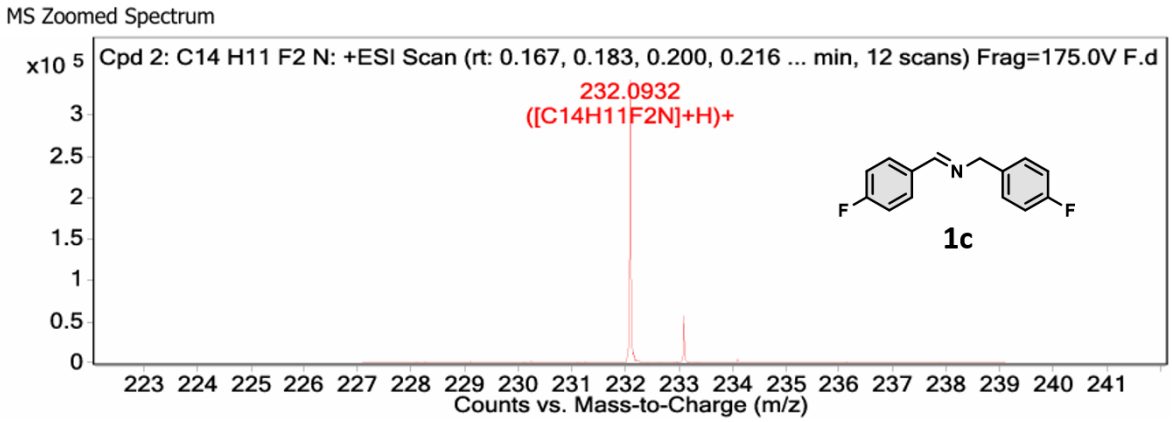

MS Spectrum Peak List

m/z	*Calc m/z*	Diff(ppm)	z	Abund	Formula	Ion
232.0932	232.0932	0.21	1	357666.53	C14H11F2N	(M+H)+
233.0964	233.0965	0.19	1	56962.28	C14H11F2N	(M+H)+
234.0995	234.0997	0.97	1	4272.5	C14H11F2N	(M+H)+

Figure S28 HRMS data for 1c

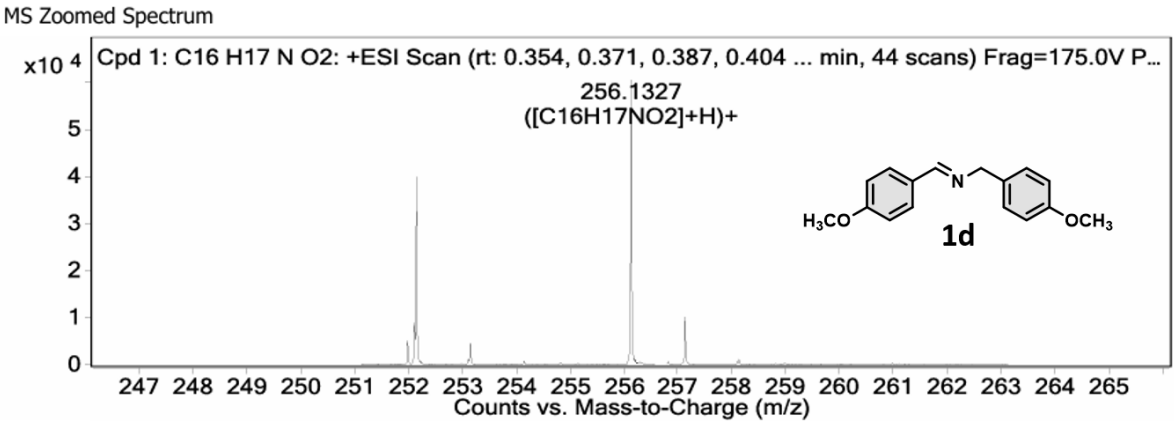

MS Spectrum Peak List

m/z	*Calc m/z*	Diff(ppm)	z	Abund	Formula	Ion
256.1327	256.1332	2.04	1	61343.25	C16H17NO2	(M+H)+
257.1359	257.1365	2.04	1	10667.24	C16H17NO2	(M+H)+
258.1379	258.1392	5.26	1	1220.29	C16H17NO2	(M+H)+

Figure S29 HRMS data for 1d

MS Zoomed Spectrum

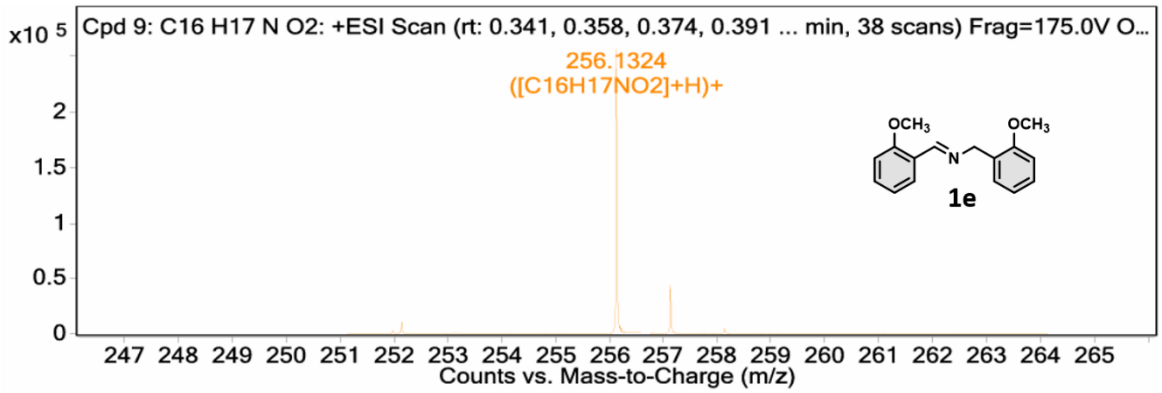

MS Spectrum Peak List

m/z	*Calc m/z*	Diff(ppm)	z	Abund	Formula	Ion
256.1324	256.1332	3.15	1	258455.63	C16H17NO2	(M+H)+
257.1355	257.1365	3.92	1	44576.36	C16H17NO2	(M+H)+
258.1384	258.1392	3.1	1	4896.12	C16H17NO2	(M+H)+
259.1409	259.1419	3.86	1	429.37	C16H17NO2	(M+H)+

Figure S30 HRMS data for 1e

MS Zoomed Spectrum

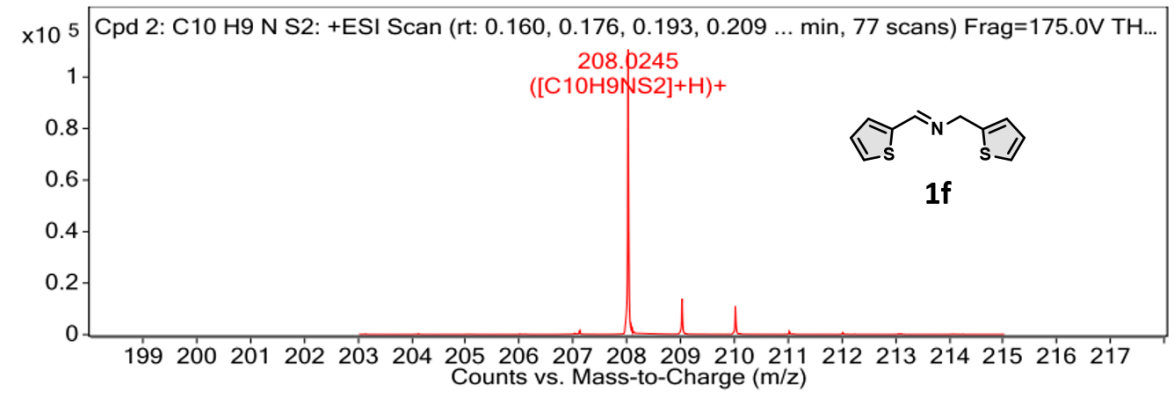

MS Spectrum Peak List

m/z	*Calc m/z*	Diff(ppm)	z	Abund	Formula	Ion
208.0245	208.0249	1.79	1	112613.94	C10H9NS2	(M+H)+
209.0273	209.0276	1.47	1	14167.99	C10H9NS2	(M+H)+
210.0207	210.0215	3.56	1	11045.97	C10H9NS2	(M+H)+

Figure S31 HRMS data for 1f

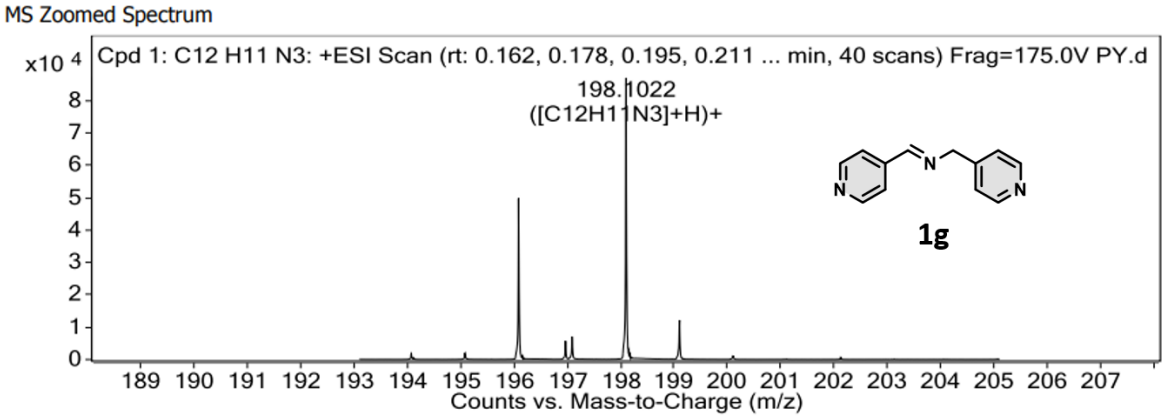

MS Spectrum Peak List

m/z	*Calc m/z*	Diff(ppm)	z	Abund	Formula	Ion
198.1022	198.1026	2.07	1	88445.86	C12H11N3	(M+H)+
199.1048	199.1055	3.22	1	12440.07	C12H11N3	(M+H)+
200.1113	200.1083	-14.69	1	1271.74	C12H11N3	(M+H)+

Figure S32 HRMS data for 1g

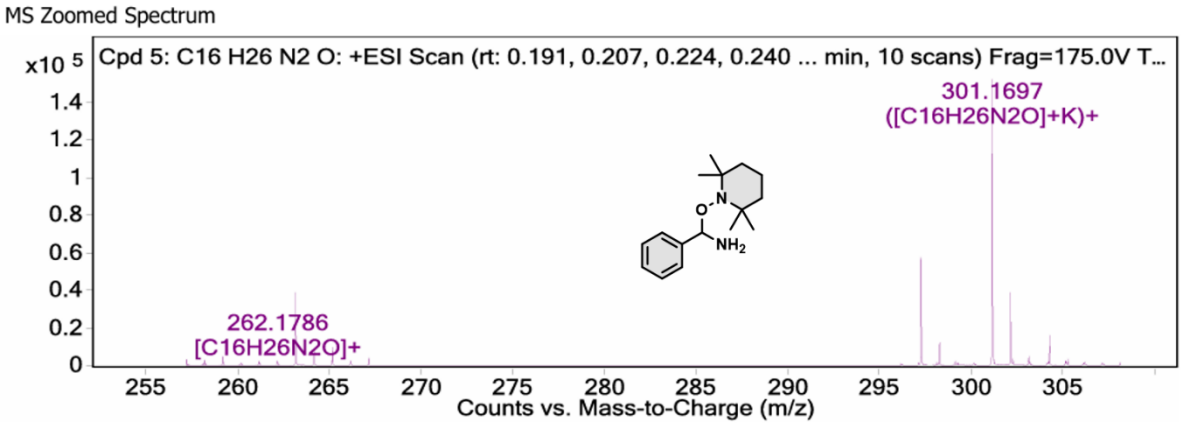

MS Spectrum Peak List

m/z	*Calc m/z*	Diff(ppm)	z	Abund	Formula	Ion
262.1786	262.204	96.93	1	1702.87	C16H26N2O	M+
301.1697	301.1677	-6.88	1	157437.94	C16H26N2O	(M+K)+
302.1726	302.1708	-6	1	39458.26	C16H26N2O	(M+K)+
303.1729	303.1674	-18.3	1	5133.03	C16H26N2O	(M+K)+

Figure S33 HRMS data for BNA-TEMPO adduct.

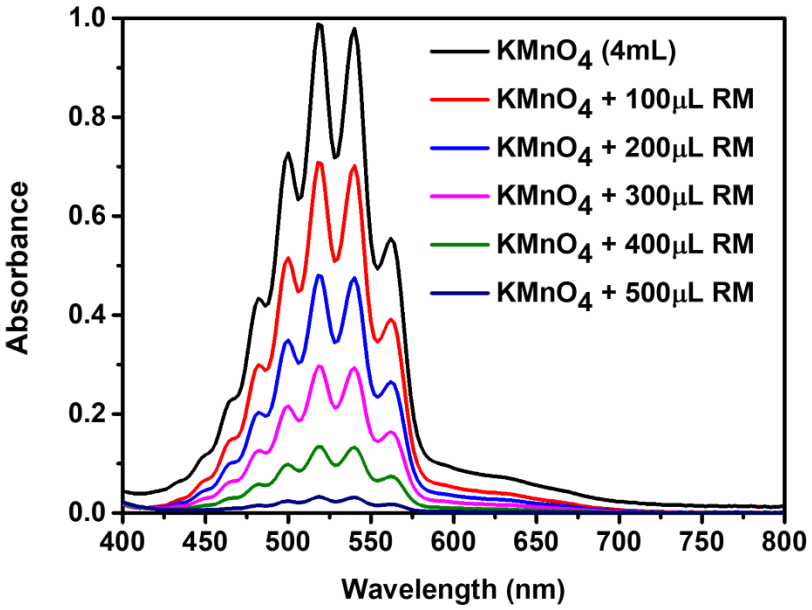

Figure S34 Detection of H_2O_2 in the reaction mixture after completion of the reaction.

RM = Reaction Mixture

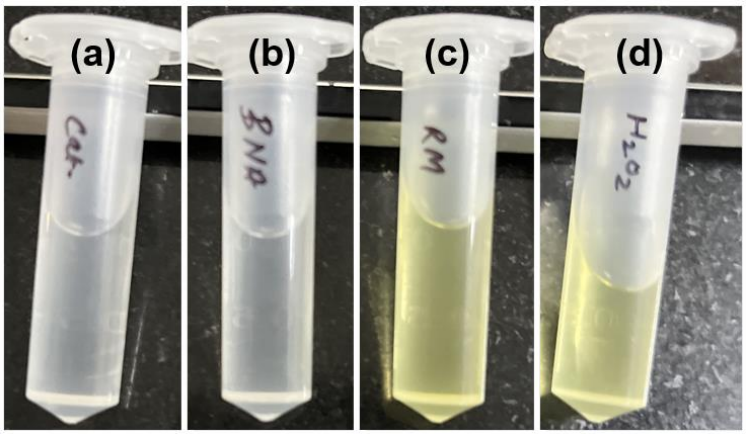

Figure S35 Detection of H_2O_2 in the photocatalytic reaction mixture by calorimetric analysis with KI solution. **(a)** KI(0.2M) + Ph-BT-Ph only **(b)** KI(0.2M) + BNA only **(c)** KI(0.2M) + RM **(d)** KI(0.2M) + H_2O_2 only. Yellow color appearance in photocatalytic reaction mixture after addition of KI solution indicating presence of H_2O_2. RM = Reaction Mixture.

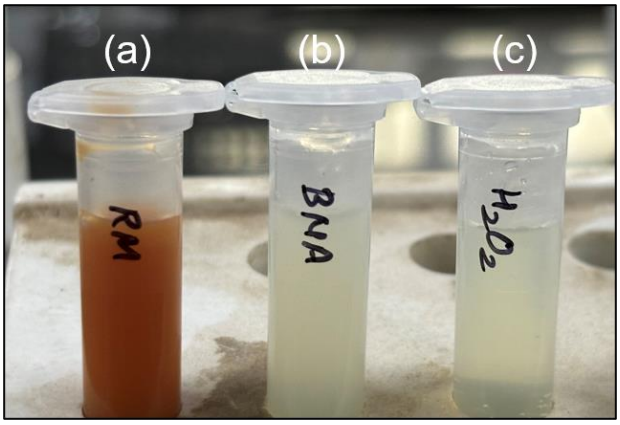

Figure S36 Nessler reagent (NR) test for ammonia detection **(a)** Aqueous layer of RM + NR **(b)** Aqueous layer of BNA + NR **(c)** Aqueous H_2O_2 + NR. Brown color appearance in aqueous layer of RM is indicating presence of NH_3 in photocatalytic reaction mixture. RM = Reaction Mixture.

Long-term Stability Test

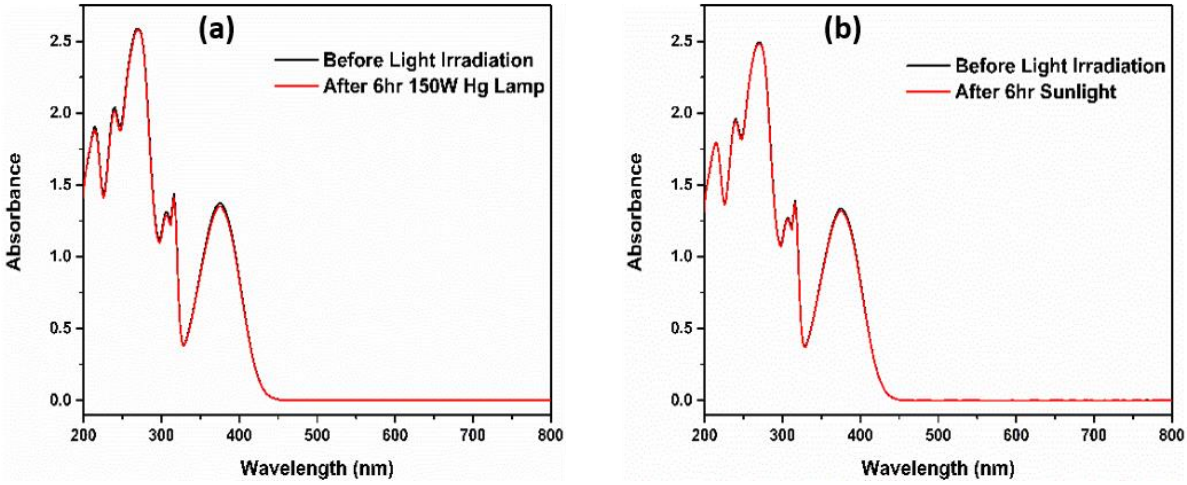

Figure S37 Long-term stability of the photocatalyst under (a) 150W Hg Lamp (b) Natural sunlight.

Reusability Study

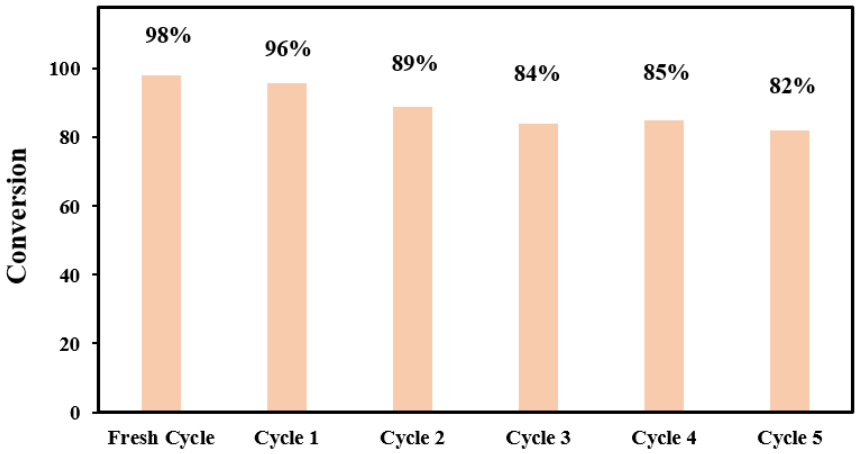

Figure S38 Reusability study of photocatalyst Ph-BT-Ph for the oxidative coupling of amines to imines for five consecutive cycle after fresh catalytic cycle performed under 250W Visible light lamp.

Details from DFT studies

The relative energetic alignment of the molecular orbitals of BNA, Ph-BT-Ph (singlet, triplet) and Oxygen molecule in triplet and singlet states are shown in Figure S37. Below we discuss the possible reactions occurring both in the electron transfer and energy transfer pathways as obtained from DFT.

Formation of BNA—[Ph-BT-Ph] complex (electron-transfer)

As proposed in the scheme shown in Figure 6, we consider that BNA molecule interacts with Ph-BT-Ph to form a loosely bound complex **BNA—[Ph-BT-Ph]**. We investigated the binding of BNA and Ph-BT-Ph using DFT and various structures were explored with BNA interactions at different configurations. The most stable structure with Ph-BT-Ph in ground state shows that the interaction of BNA and Ph-BT-Ph in singlet ground state is attractive with a negative binding energy, but the energy is small.

1) BNA + ^{1}PS-1→ **BNA—[Ph-BT-Ph]** complex, ΔE_{bind} = -0.001 eV,

It is however more likely that, the photocatalyst Ph-BT-Ph molecule exists in the excited state during interaction with BNA as the reaction occurs in presence of sunlight, therefore we studied the complex formation with singlet excited state and triplet of Ph-BT-Ph as below. We optimized the structure of Ph-BT-Ph in singlet excited state S1, which was a stable structure and estimated the binding energy for complex formation with BNA. The binding energy is negative, and binding is stronger compared to the interaction with the ground state given above.

2) BNA + **Ph-BT-Ph** (S1 state)→ **BNA—[Ph-BT-Ph]** complex, ΔE_{bind} = -0.0137 eV,

The binding energy of BNA with triplet Ph-BT-Ph was also calculated:

3) BNA + ^{3}Ph-BT-Ph → **BNA—[Ph-BT-Ph]** complex, ΔE_{bind} = -0.064 eV,

Considering the above three cases we conclude that formation of BNA complex with the photocatalyst is more probable when Ph-BT-Ph is in excited state. The **BNA—[Ph-BT-Ph]** complex thus formed can pave the way of electron transfer from BNA to Ph-BT-Ph in the excited state, which acts as a mediator for electron transfer.

The changes in the bond distances for the ground state (GS) and the excited state (ES, S1) of Ph-BT-Ph have been tabulated in Table S2. The structure of Ph-BT-Ph is not fully planer as with the central ring out-of-plane, as shown in Figure S37. In excited state S1, not only the N-S and C-C bond-distances of the central portion changed, but the dihedral angles also changed, which is an indicator of planarity (shown in Table S2).

We then considered the interaction of **BNA—[Ph-BT-Ph]** complex with ROS, singlet oxygen ($^1O_2$) to form BNA-OOH while the photocatalyst Ph-BT-Ph is regenerated. The reaction is thermodynamically favourable with a negative free energy as shown here. The free energies of other reactions are also listed below.

4) **BNA—[Ph-BT-Ph]** complex + $^1O_2$ → BNA-OOH + Ph-BT-Ph, ΔG_{ACN} =-0.089 eV

5) BNA-OOH → Ph−CH=NH + H_2O_2, ΔG_{ACN}= -0.20 eV

Further reaction-steps with BNA to produce NH_3 and BNI in two consecutive steps are shown which have slightly negative free energy.

6) Ph−CH=NH + BNA → BNI + NH_3, ΔG_{ACN}=-0.18 eV

Formation of [Ph-BT-Ph]—O_2 complex (energy-transfer)

The calculated electronic energy difference between the Ph-BT-Ph in singlet, ground state and excited, triplet state is 1.85 eV which is already shown in Figure 7d.

7) Ph-BT-Ph + hυ $\rightarrow$ ^{1}Ph-BT-Ph * (singlet excited state) $\rightarrow$ ^{3}Ph-BT-Ph (triplet state)

We now consider below the oxygen binding with triplet Ph-BT-Ph to form complex [**Ph-BT-Ph**]—**O_2,** which produces ROS, $^{1}O_2$ and the photocatalyst is regenerated**.** Then ROS can again react with BNA—[Ph-BT-Ph] complex, and reaction 4, 5 and 6 can take place forming final products within the reaction mixture. The oxygen binding energy to the triplet photocatalyst is negative.

8) ^{3}Ph-BT-Ph + $^{3}O_2$ $\rightarrow$ [**Ph-BT-Ph**]—**O_2** (Ph-BT-Ph oxygen complex), E_{bind} = -0.25 eV,

9) **[Ph-BT-Ph]—O_2** complex $\rightarrow$ Ph-BT-Ph + $^{1}O_2$ (singlet O_2), ΔG_{ACN} = 0.0091 eV,

The overall reaction considering the electron transfer and energy transfer pathways is the interaction of the two complexes, namely the **BNA—[Ph-BT-Ph]** and **[Ph-BT-Ph]—O_2** in excess BNA and in presence of sunlight forms BNI, H_2O_2 and NH_3 with two molecules of catalyst being regenerated.

10) **BNA—[Ph-BT-Ph]** + **[Ph-BT-Ph]—O_2** + BNA$\rightarrow$2Ph-BT-Ph + BNI + NH_3 + H_2O_2, ΔG_{ACN} = -0.11 eV

We also studied the optimized structure of excited state S6 as the TD-DFT spectrum shows the highest oscillator strength for this transition.

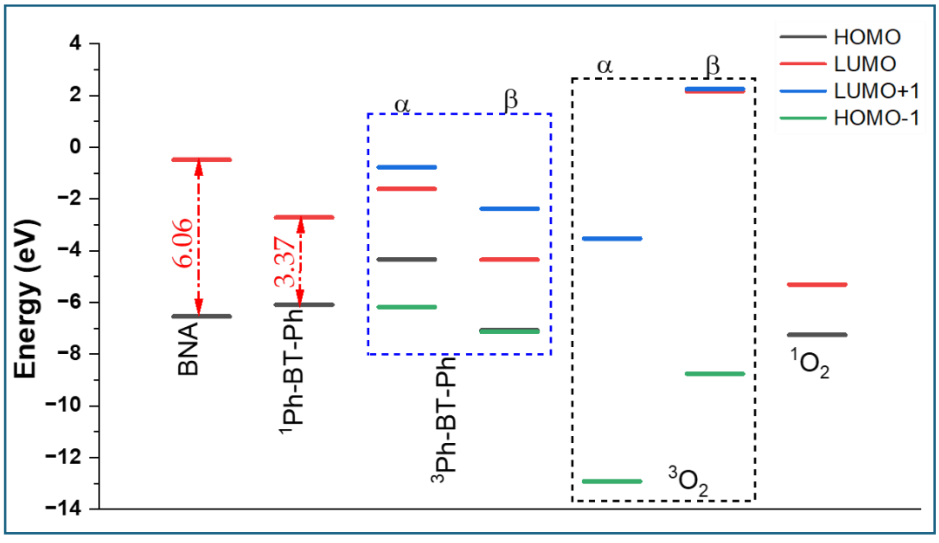

Figure S39 The relative energetic alignment of the molecular orbitals of BNA, Ph-BT-Ph (singlet, triplet) and Oxygen molecule in triplet and singlet states.

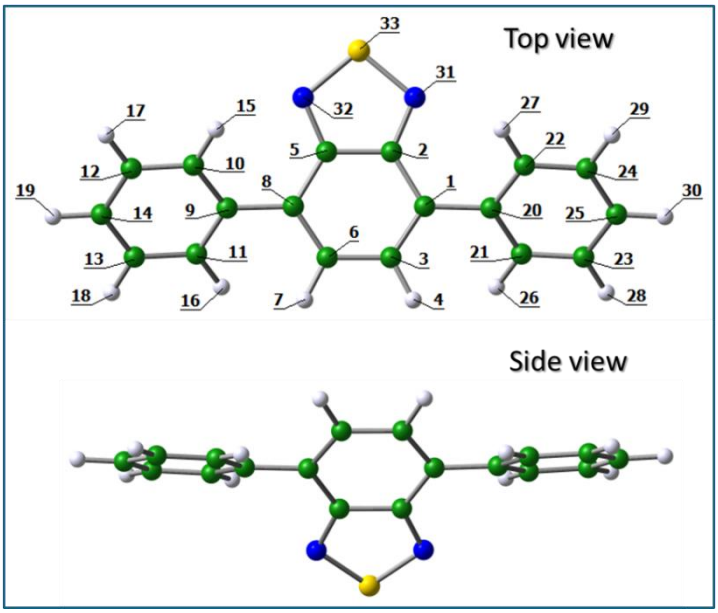

Figure S40 Structure of Ph-BT-Ph shown with atom numbers marked. The overall planarity of the structure is clear in the top and side views.

Table S2 Few important bond distances in Å are tabulated in ground and excited states, S1 and S6. Two dihedral angles are given to show the changes in planarity in the ground and excited states.

Bond-distance/ Dihedral angle	**Ground state GS**	**Excited state ES, S1**	**Excited state ES, S6**
33-31	1.64	1.68	1.67
33-32	1.64	1.68	1.67
32-5	1.33	1.34	1.35
31-2	1.33	1.34	1.35
5-2	1.46	1.45	1.51
5-8	1.43	1.44	1.42
2-1	1.43	1.44	1.42
8-6	1.38	1.43	1.40
1-3	1.38	1.43	1.40
6-3	1.42	1.37	1.42
9-8	1.48	1.45	1.475
1-20	1.48	1.45	1.475
2-1-20-22 (degree)	42.4	22.6	36
5-8-9-11 (degree)	139.1	158.4	145.6

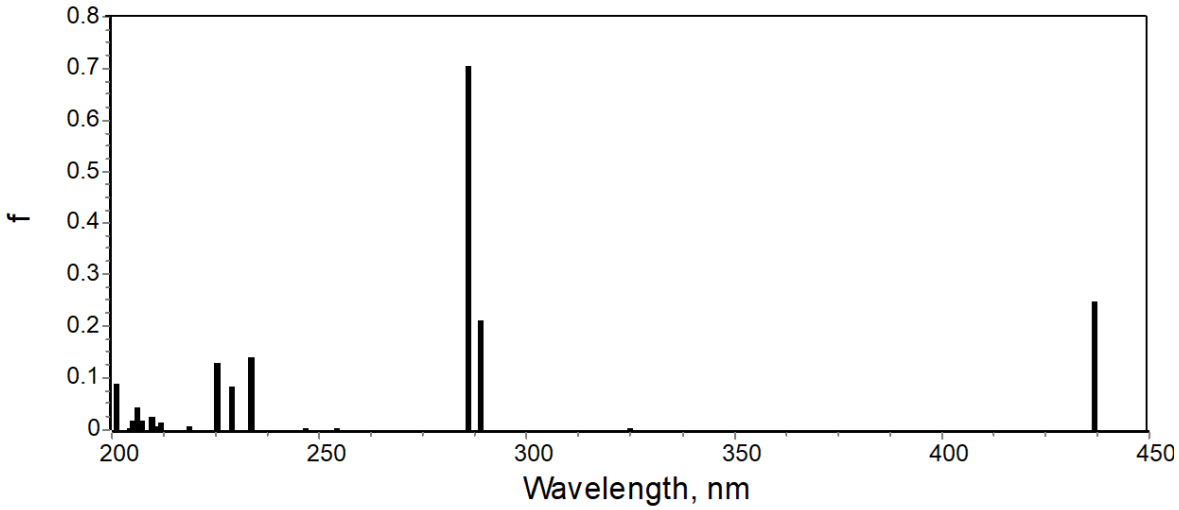

Figure S41 Calculated electronic spectrum in acetonitrile (ACN) obtained from TD-DFT studies.

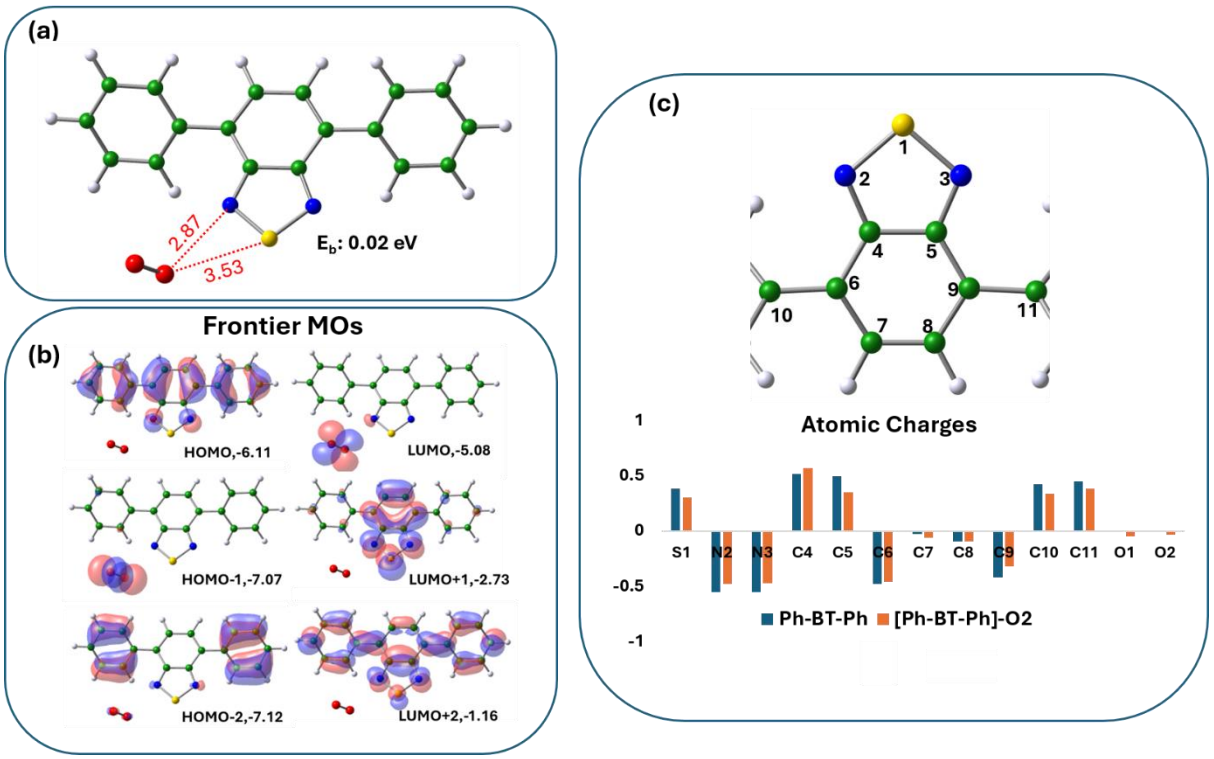

Figure S42 (a) The optimized structure of Ph-BT-Ph--O_2 complex with oxygen bound in side-on position interacting preferentially with N atoms of the benzothiadiazole ring. **(b)** Plots of frontier molecular orbitals including the HOMO and LUMO of Ph-BT-Ph--O_2 complex, the color codes show different signs of wavefunctions. The energies of the respective MOs in the eV are written alongside. **(c)** Bar chart showing the changes in atomic charges of Ph-BT-Ph before and after interaction with Oxygen.

Optimized Co-ordinates for structures reported

Ph-BT-Ph (Ground state)

B3LYP/6-311+G** (SMD, solvent=acetonitrile)

C	1.469209000	-0.514567000	0.071958000
C	0.728109000	0.701128000	-0.114311000
C	0.711054000	-1.654689000	0.224525000
H	1.212458000	-2.602372000	0.383680000
C	-0.728109000	0.701128000	-0.114311000
C	-0.711055000	-1.654689000	0.224525000
H	-1.212458000	-2.602372000	0.383680000
C	-1.469209000	-0.514566000	0.071958000
C	-2.951070000	-0.551225000	0.089348000
C	-3.701501000	0.423507000	0.767447000
C	-3.637622000	-1.594195000	-0.554189000
C	-5.092130000	0.350164000	0.806563000
C	-5.028626000	-1.662823000	-0.517761000
C	-5.762231000	-0.691193000	0.163483000
H	-3.195312000	1.231836000	1.279485000
H	-3.079473000	-2.346497000	-1.099987000
H	-5.652598000	1.107694000	1.343657000
H	-5.538958000	-2.472416000	-1.028106000
H	-6.845056000	-0.743673000	0.191217000
C	2.951070000	-0.551226000	0.089348000
C	3.637622000	-1.594195000	-0.554188000
C	3.701501000	0.423507000	0.767447000
C	5.028626000	-1.662824000	-0.517761000
C	5.092130000	0.350164000	0.806563000
C	5.762230000	-0.691193000	0.163483000
H	3.079473000	-2.346498000	-1.099987000
H	3.195312000	1.231836000	1.279484000
H	5.538959000	-2.472416000	-1.028106000
H	5.652597000	1.107694000	1.343656000
H	6.845056000	-0.743673000	0.191217000
N	1.250249000	1.910055000	-0.343398000
N	-1.250249000	1.910055000	-0.343398000
S	0.000000000	2.952301000	-0.536068000

Ph-BT-Ph (Excited state S1)

B3LYP/6-311+G** (SMD, solvent=acetonitrile)

C	1.462535000	-0.455999000	0.052374000
C	0.724830000	0.779636000	0.090173000
C	0.685326000	-1.655928000	-0.004843000
H	1.193091000	-2.610294000	0.007873000
C	-0.724830000	0.779636000	0.090173000
C	-0.685326000	-1.655928000	-0.004843000
H	-1.193091000	-2.610295000	0.007873000
C	-1.462535000	-0.455999000	0.052373000
C	-2.910881000	-0.533410000	0.073300000
C	-3.721654000	0.513640000	0.591380000
C	-3.577920000	-1.692904000	-0.415181000
C	-5.102417000	0.398775000	0.624248000
C	-4.958411000	-1.788899000	-0.395505000
C	-5.732561000	-0.746676000	0.128122000
H	-3.248174000	1.401180000	0.982123000
H	-3.006626000	-2.505266000	-0.844187000
H	-5.695565000	1.204801000	1.041499000
H	-5.440008000	-2.675569000	-0.791969000
H	-6.813436000	-0.828355000	0.149584000
C	2.910881000	-0.533410000	0.073301000
C	3.577920000	-1.692904000	-0.415181000
C	3.721654000	0.513639000	0.591381000
C	4.958411000	-1.788899000	-0.395506000
C	5.102417000	0.398774000	0.624248000
C	5.732561000	-0.746676000	0.128122000
H	3.006625000	-2.505265000	-0.844187000
H	3.248175000	1.401180000	0.982124000
H	5.440008000	-2.675569000	-0.791970000
H	5.695565000	1.204801000	1.041499000
H	6.813436000	-0.828356000	0.149584000
N	1.271079000	2.006959000	0.069806000
N	-1.271079000	2.006959000	0.069806000
S	0.000000000	3.110391000	0.073559000

[Ph-BT-Ph]—O_2 complex (bridge)

B3LYP/6-311+G** (SMD, solvent=acetonitrile)

C	-1.466580000	-0.370330000	-0.339929000
C	-0.725755000	0.826776000	-0.030132000
C	-0.702681000	-1.479267000	-0.687932000
H	-1.209242000	-2.390978000	-0.979694000
C	0.725902000	0.826723000	-0.030024000
C	0.702820000	-1.479273000	-0.687964000
H	1.209353000	-2.390992000	-0.979751000
C	1.466712000	-0.370403000	-0.339871000

C	2.942898000	-0.417527000	-0.357280000
C	3.707930000	0.662191000	-0.831901000
C	3.612497000	-1.578247000	0.069227000
C	5.096741000	0.576818000	-0.884215000
C	5.001280000	-1.654549000	0.026390000
C	5.749371000	-0.577865000	-0.452042000
H	3.215474000	1.560274000	-1.179466000
H	3.043669000	-2.416023000	0.454740000
H	5.669492000	1.414994000	-1.265486000
H	5.499682000	-2.553537000	0.371789000
H	6.831505000	-0.638394000	-0.486864000
C	-2.942757000	-0.417439000	-0.357382000
C	-3.612370000	-1.578132000	0.069175000
C	-3.707769000	0.662269000	-0.832056000
C	-5.001155000	-1.654417000	0.026338000
C	-5.096581000	0.576911000	-0.884373000
C	-5.749227000	-0.577744000	-0.452149000
H	-3.043554000	-2.415895000	0.454734000
H	-3.215298000	1.560330000	-1.179659000
H	-5.499572000	-2.553380000	0.371777000
H	-5.669319000	1.415077000	-1.265687000
H	-6.831362000	-0.638260000	-0.486975000
N	-1.249078000	1.999134000	0.328374000
N	1.249255000	1.999050000	0.328533000
S	0.000099000	3.015963000	0.634650000
O	0.620647000	-1.127971000	2.080105000
O	-0.622059000	-1.128890000	2.079208000

[Ph-BT-Ph]—O_2 complex (side-on)
B3LYP/6-311+G** (SMD, solvent=acetonitrile)

C	1.920928000	-0.639322000	0.047366000
C	1.004739000	0.465480000	0.005565000
C	1.343192000	-1.889123000	0.088189000
H	1.982517000	-2.763218000	0.133054000
C	-0.435185000	0.249676000	0.030695000
C	-0.062988000	-2.100045000	0.112478000
H	-0.415908000	-3.122890000	0.175443000
C	-0.983393000	-1.075307000	0.098006000
C	-2.442363000	-1.334452000	0.137662000
C	-3.297794000	-0.580817000	0.957555000
C	-2.994378000	-2.373850000	-0.628940000
C	-4.660601000	-0.864725000	1.013206000
C	-4.358494000	-2.652383000	-0.575863000
C	-5.197454000	-1.899350000	0.246043000
H	-2.892898000	0.216913000	1.567371000
H	-2.353812000	-2.955796000	-1.282122000
H	-5.303390000	-0.277743000	1.660295000
H	-4.766171000	-3.453846000	-1.182350000

H	-6.259383000	-2.115339000	0.287090000
C	3.391971000	-0.456291000	0.032282000
C	4.199719000	-1.305245000	-0.742403000
C	4.015640000	0.536313000	0.806157000
C	5.586180000	-1.168443000	-0.741129000
C	5.402516000	0.667628000	0.810003000
C	6.193840000	-0.181814000	0.035808000
H	3.737974000	-2.065927000	-1.361868000
H	3.415451000	1.196132000	1.419735000
H	6.190754000	-1.828991000	-1.353115000
H	5.865568000	1.433912000	1.422229000
H	7.272938000	-0.074343000	0.036504000
N	1.337388000	1.755348000	-0.104310000
N	-1.133940000	1.385719000	-0.062732000
S	-0.054824000	2.616853000	-0.166598000
O	-3.283336000	3.290312000	-0.050003000
O	-4.063795000	3.155493000	-0.960435000

BNA—[Ph-BT-Ph] complex
B3LYP/6-311+G** (SMD, solvent=acetonitrile)

C	2.619375000	-0.608192000	-0.420455000
C	1.727940000	-0.442729000	0.692817000
C	2.094950000	-1.273015000	-1.506882000
H	2.722719000	-1.442642000	-2.374005000
C	0.371233000	-0.970904000	0.655512000
C	0.772137000	-1.793790000	-1.541316000
H	0.469459000	-2.332447000	-2.431827000
C	-0.115420000	-1.681451000	-0.493527000
C	-1.480226000	-2.256273000	-0.560251000
C	-2.049132000	-2.925391000	0.535991000
C	-2.223911000	-2.169631000	-1.748835000
C	-3.316384000	-3.496260000	0.440713000
C	-3.492840000	-2.737182000	-1.840279000
C	-4.044734000	-3.403666000	-0.745871000
H	-1.492487000	-3.013874000	1.460203000
H	-1.812120000	-1.640626000	-2.600767000
H	-3.734039000	-4.016709000	1.295773000
H	-4.052898000	-2.651933000	-2.765176000
H	-5.032936000	-3.844729000	-0.816322000
C	4.008937000	-0.091544000	-0.413624000
C	4.537736000	0.522940000	-1.560826000
C	4.837002000	-0.228191000	0.712758000
C	5.852755000	0.982733000	-1.582621000
C	6.153162000	0.227730000	0.686822000
C	6.666669000	0.836378000	-0.459052000
H	3.910213000	0.655773000	-2.434911000
H	4.455657000	-0.707503000	1.605420000
H	6.238672000	1.461500000	-2.476044000
H	6.779471000	0.103891000	1.563647000

H	7.690038000	1.194734000	-0.475337000
N	2.000570000	0.218131000	1.822204000
N	-0.329985000	-0.685498000	1.757820000
S	0.654160000	0.168002000	2.754469000
C	-3.233347000	2.547435000	0.445752000
C	-1.934693000	3.046476000	0.287930000
C	-4.089923000	2.553255000	-0.663528000
C	-1.497582000	3.530033000	-0.946369000
C	-3.658108000	3.035449000	-1.898805000
C	-2.358148000	3.524108000	-2.044533000
H	-1.261636000	3.060534000	1.140002000
H	-5.104236000	2.179655000	-0.556918000
H	-0.488298000	3.914794000	-1.048752000
H	-4.336241000	3.035507000	-2.745795000
H	-2.021642000	3.901932000	-3.003965000
N	-3.598807000	0.507982000	1.893449000
C	-3.693638000	1.975889000	1.774784000
H	-4.736519000	2.256052000	1.948773000
H	-3.102093000	2.415651000	2.582188000
H	-2.636570000	0.205491000	1.752124000
H	-4.146367000	0.067369000	1.158070000

Table S3 Comparison with the existing literature based on benzothiadiazole for oxidative coupling of amines to imines.

S.No.	Catalyst	Light Source	Amount of Catalyst	Reactant Amount	Time	Conversion	Reference
1	B-BT	Blue LED 460nm	3mg	1mmol	3hr	74%	[9][9]
2	CMP-BT@P-PAN	Visible light (22 W/m^2 , $\lambda > 450$ nm)	50mg	0.02mmol	1hr	95%	[10][10]
3	Py-BSZ-COF	15 W 520 nm LED bulb (5 mW cm^{-2})	5mg	0.2mmol	12hr	99%	[11][11]
4	BTDA−TAPT	300 W Xe lamp (λ = 420−780 nm)	6mg	0.1mmol	6hr	97%	[12][12]
5	Tp-BTD-ABC	Blue LED 460nm (3W × 4)	5mg	0.3mmol	40min	72%	[13][13]
6	ClBD-BTT	300 W Xe Lamp	10mg	2mmol	6hr	82%	[14][14]
7	Tp-BTD-25	Blue LEDs (3 W × 4)	5mg	0.3mmol	0.5hr	94%	[15][15]
8	JNU-207	Blue LED	1mol%	2eq.	24hr	94% yield	[16][16]
9	JNU-211	Blue LED	4mg	0.5mmol	12h	99%	[17][17]
10	TBP	45W LED ($\lambda > 400$ nm)	15mg	1mmol	2hr	>99%	[18][18]
11	1-Zn	10 W Blue LED lamp (465 nm, 2252 mW/cm^2)	5mg	0.2mmol	2.5hr	99% yield	[19][19]
12	UiO-68-BT	415 nm LEDs (3 W × 4)	5mg	0.3mmol	25min	96%	[20][20]
13	PY-BT COF	300W Xenon lamp (200 mW cm^{-2})	5mg	0.1mmol	2.5hr	99.9%	[21][21]
14	**Ph-BT-Ph***	**Natural Sunlight**	**0.13mol% OR 75µg**	**0.2mmol**	**2hr**	**>99% TOF* = 381 h^{-1}**	**This work**

Table S4 Comparison with the existing literature for oxidative coupling of amines to imines in natural sunlight/xenon lamp/blue LED other than benzothiadiazole based system.

S.No.	Catalyst	Light Source	Amount of Catalyst	Reactant Amount	Time	Conversion	Reference
1	TiO_2/BiOBr	Natural Sunlight	0.1g	0.125mmol	1hr	89.9%	[22][22]
2	$WO_3.H_2O$/Pd/CdS	Simulated Sunlight ($360 \leq \lambda \leq 780$ nm)	6mg	0.05mmol	2hr	95%	[23][23]
3	CWOH-1	Natural Sunlight	20mg	0.1mmol	7hr	94%	[24][24]
4	Tx-CMP	Natural Sunlight	10mg	0.5mmol	4hr	>99%, TOF = 12.4	[25][25]
5	CeR-CN-66%	Xenon Arc Lamp	50mg	100mg	5hr	82.2%	[26][26]
6	3*	Natural Sunlight	0.25mol%	0.5mmol	1hr	>99%	[27][27]
7	TPT-porp	Natural Sunlight	5mg	0.1mmol	6hr	65%	[28][28]
8	Ag_3PO_4	Natural Sunlight	25mg	1mmol	40min	95%, TOF* = 57 h^{-1}	[29][29]
11	(Au NBP)/t-TiO_2	Xe lamp	10mg	0.1mmol	8hr	91.9%	[30][30]
12	1	Xe Lamp Cutoff filter (AM 1.5G, 100 mW cm^{-2})	1mol%	0.2mmol	24hr	96% yield	[31][31]
13	SAD	Natural sunlight	15mg	0.2mmol	6hr	38%	[32][32]
14	PAA-CMP	Natural Sunlight	100mg	18.7mmol	48hr	65% yield	[33][33]
15	eosin Y*	Sunlight lamp (1000 Wm^{-2})	1.5mol%	5mM	1hr	89%, TOF* = 192 h^{-1}	[34][34]
16	C-CMP	150 W Xe lamp	20mg	1mmol	4hr	>99%	[35][35]
17	Au/SnS2 NSs	Sunlight	15mg	0.2mmol	90min	98%	[36][36]
18	1l*	10 W Blue LED	10mol%	0.5mmol	16hr	95% yield	[37][37]
19	CD_1	Xe light Natural Sunlight	15mg 15mg	0.5mmol 0.5mmol	60min 60min	96%, TOF=32 90%, TOF=30	[38][38]
20	**Ph-BT-Ph***	**Natural Sunlight**	**0.13mol% OR 75µg**	**0.2mmol**	**2hr**	**>99% TOF* = 381 h^{-1}**	**This work**

- (* in catalyst) Indicating homogenous system.
- TOF* = mmol of benzylamine converted per mmol of catalyst per hour.
- TOF = mmol of benzylamine converted per gram of catalyst per hour.

References:

1. M. J. Frisch, G. W. Trucks, H. B. Schlegel, G. E. Scuseria, M. A. Robb, J. R. Cheeseman, G. Scalmani, V. Barone, G. A. Petersson, H. Nakatsuji, X. Li, M. Caricato, A. V. Marenich, J. Bloino, B. G. Janesko, R. Gomperts, B. Mennucci, H. P. Hratchian, J. V. Ortiz, A. F. Izmaylov, J. L. Sonnenberg, Williams, F. Ding, F. Lipparini, F. Egidi, J. Goings, B. Peng, A. Petrone, T. Henderson, D. Ranasinghe, V. G. Zakrzewski, J. Gao, N. Rega, G. Zheng, W. Liang, M. Hada, M. Ehara, K. Toyota, R. Fukuda, J. Hasegawa, M. Ishida, T. Nakajima, Y. Honda, O. Kitao, H. Nakai, T. Vreven, K. Throssell, J. A. Montgomery Jr., J. E. Peralta, F. Ogliaro, M. J. Bearpark, J. J. Heyd, E. N. Brothers, K. N. Kudin, V. N. Staroverov, T. A. Keith, R. Kobayashi, J. Normand, K. Raghavachari, A. P. Rendell, J. C. Burant, S. S. Iyengar, J. Tomasi, M. Cossi, J. M. Millam, M. Klene, C. Adamo, R. Cammi, J. W. Ochterski, R. L. Martin, K. Morokuma, O. Farkas, J. B. Foresman and D. J. Fox, *Journal*, 2016.
2. A. D. Becke, *J. Chem. Phys.,* 1993, **98**, 5648-5652.
3. C. Lee, W. Yang and R. G. Parr, *Phys. Rev. B,* 1988, **37**, 785-789.
4. S. H. Vosko, L. Wilk and M. Nusair, *Can. J. Phys.,* 1980, **58**, 1200-1211.
5. B. H. Besler, K. M. Merz Jr and P. A. Kollman, *J. Comput. Chem.,* 1990, **11**, 431-439.
6. U. C. Singh and P. A. Kollman, *J. Comput. Chem.,* 1984, **5**, 129-145.
7. Y. Zhao, N. E. Schultz and D. G. Truhlar, *J. Chem. Theory Comput.,* 2006, **2**, 364-382.
8. A. V. Marenich, C. J. Cramer and D. G. Truhlar, *J. Phys. Chem. B,* 2009, **113**, 6378-6396.
9. Z. J. Wang, K. Garth, S. Ghasimi, K. Landfester and K. A. I. Zhang, *ChemSusChem*, 2015, **8**, 3459-3464.
10. J. J. Lee, W. Noh, T.-H. Huh, Y.-J. Kwark and T. S. Lee, *Polymer*, 2020, **211**, 123060.
11. S. Li, L. Li, Y. Li, L. Dai, C. Liu, Y. Liu, J. Li, J. Lv, P. Li and B. Wang, *ACS Catal.,* 2020, **10**, 8717-8726.
12. Q. Li, J. Wang, Y. Zhang, L. Ricardez-Sandoval, G. Bai and X. Lan, *ACS Appl. Mater. Interfaces.,* 2021, **13**, 39291-39303.
13. S. Yang, X. Li, Y. Qin, Y. Cheng, W. Fan, X. Lang, L. Zheng and Q. Cao, *ACS Appl. Mater. Interfaces.,* 2021, **13**, 29471-29481.
14. C. Chu, Y. Qin, C. Ni and J. Zou, *Chin. Chem. Lett.,* 2022, **33**, 2736-2740.
15. X. Li, S. Yang, F. Zhang, L. Zheng and X. Lang, *Appl. Catal. B: Environ.,* 2022, **303**, 120846.

16. K. Wu, J.-K. Jin, X.-Y. Liu, Y.-L. Huang, P.-W. Cheng, M. Xie, J. Zheng, W. Lu and D. Li, *J. Mater. Chem. C,* 2022, **10**, 11967-11974.
17. K. Wu, X.-Y. Liu, M. Xie, P.-W. Cheng, J. Zheng, W. Lu and D. Li, *Appl. Catal. B: Environ.,* 2023, **334**, 122847.
18. S. Ahmed, A. Kumar and P. S. Mukherjee, *ChemComm.,* 2023, **59**, 3229-3232.
19. Q.-Q. Li, P.-H. Pan, H. Liu, L. Zhou, S.-Y. Zhao, B. Deng, Y.-J. He, J.-X. Song, P. Liu, Y.-Y. Wang and J.-L. Li, *Inorg. Chem.,* 2023, **62**, 17182-17190.
20. B. Zeng, Y. Wang, F. Huang, K. Xiong, K. Zhang and X. Lang, *Catal. Sci. Technol.,* 2024, **14**, 2838-2847.
21. M.-Y. Yang, S.-B. Zhang, M. Zhang, Z.-H. Li, Y.-F. Liu, X. Liao, M. Lu, S.-L. Li and Y.-Q. Lan, *J. Am. Chem. Soc.,* 2024, **146**, 3396-3404.
22. S. Juntrapirom, D. Tantraviwat, O. Thongsook, S. Anuchai, S. Pornsuwan, D. Channei and B. Inceesungvorn, *Appl. Surf. Sci.,* 2021, **545**, 149015.
23. R. Wang, G. Qiu, Y. Xiao, X. Tao, W. Peng and B. Li, *J. Catal.,* 2019, **374**, 378-390.
24. Z. Yue, Y. Yu, T. Hu, Y. Wang, L. Cao, Y. Zhang, Y. Chang, L. Pei and J. Jia, *Mater. Today Chem.,* 2024, **36**, 101932.
25. V. R. Battula, H. Singh, S. Kumar, I. Bala, S. K. Pal and K. Kailasam, *ACS Catal.,* 2018, **8**, 6751-6759.
26. Y. Chai, L. Zhang, Q. Liu, F. Yang and W.-L. Dai, *ACS Sustain. Chem. Eng.,* 2018, **6**, 10526-10535.
27. J. Zhou, L. Mao, M.-X. Wu, Z. Peng, Y. Yang, M. Zhou, X.-L. Zhao, X. Shi and H.-B. Yang, *Chem. Sci.,* 2022, **13**, 5252-5260.
28. N. Saini, N. Sharma, D. K. Chauhan, R. Khurana, M. E. Ali and K. Kailasam, *J. Mater. Chem. A,* 2023, **11**, 25743-25755.
29. R. Garg, S. Mondal, L. Sahoo, C. P. Vinod and U. K. Gautam, *ACS Appl. Mater. Interfaces.,* **12**, 29324-29334.
30. G. He, Y. Lai, Y. Guo, H. Yin, B. Chang, M. Liu, S. Zhang, B. Yang and J. Wang, *ACS Appl. Mater. Interfaces.,* 2022, **14**, 53724-53735.
31. S. Li, G. Li, P. Ji, J. Zhang, S. Liu, J. Zhang and X. Chen, *ACS Appl. Mater. Interfaces.,* 2019, **11**, 43287-43293.
32. S. Mandal, B. Kommula and S. Bhattacharyya, *ACS Sustain. Chem. Eng.,* 2023, **11**, 14921-14931.
33. J. Jiang, X. Liu and R. Luo, *Catal. Lett.,* 2021, **151**, 3145-3153.

34. J. D. Tibbetts, D. R. Carbery and E. A. C. Emanuelsson, *ACS Sustain. Chem. Eng.,* 2017, **5**, 9826-9835.
35. C. Su, R. Tandiana, B. Tian, A. Sengupta, W. Tang, J. Su and K. P. Loh, *ACS Catal.,* 2016, **6**, 3594-3599.
36. S. Mondal, L. Sahoo, C. P. Vinod and U. K. Gautam, *Appl. Catal. B: Environ.,* 2021, **286**, 119927.
37. J. Zhao, H. Sun, Y. Lu, J. Li, Z. Yu, H. Zhu, C. Ma, Q. Meng and X. Peng, *Green Chem.,* 2022, **24**, 8503-8511.
38. B. Kommula, S. Chakraborty, M. Banoo, R. S. Roy, S. Sil, A. Swarnkar, B. Rawat, K. Kailasam and U. K. Gautam, *ACS Appl. Mater. Interfaces.,* 2024, **16**, 39470-39481.